

A SPATIAL ANALYSIS OF GULLIES ON MARS

THESIS

Presented to the Graduate Council
of Texas State University – San Marcos
in Partial Fulfillment
of the Requirements

for the Degree

Master of Applied Geography

by Leon Kincy, B.A., B.S.

San Marcos, Texas
December 2009

A SPATIAL ANALYSIS OF GULLIES ON MARS

Committee Members Approved:

Nathan Currit, Chair

David Butler

Sven Fuhrmann

Approved:

J. Michael Willoughby
Dean of the Graduate College

COPYRIGHT

by

Leon Kincy

2009

ACKNOWLEDGEMENTS

I wish to thank my thesis committee Dr. David Butler, Dr. Sven Fuhrmann, and my chairman Dr. Nate Currit. I am grateful to Dr. Mark Fonstad for helping me to get started on this project. I want to thank Texas State University-San Marcos and the greatest geography department in the country for allowing me to be a part of the department. I am grateful to Trent Hare of the USGS for all of his assistance with mapping, on this project. I dedicate this thesis to my parents Leondres Jr. and Geneva Cyphers Kincy.

This manuscript was submitted on June 19, 2009.

TABLE OF CONTENTS

	Page
ACKNOWLEDGEMENTS	iv
LIST OF TABLES.....	vii
LIST OF FIGURES	viii
ABSTRACT.....	x
CHAPTER	
1. INTRODUCTION	1
Geologic History of Mars	3
History of Research on Mars	4
2. LITERATURE REVIEW	8
Gully Formation.....	9
Gully Fluid Sources and Obliquity	10
Martian Surface Composition.....	15
Gully Orientation.....	17
Atmospheric and Water Cycles	19
Spatial Distribution.....	20
Objective.....	21
3. DATA AND METHODS	21
Study Area	22
Data Collection.....	22
Data Limitations and Assumptions	23
Preprocessing and Information Extraction	24
Statistical Methods	25
4. RESULTS	26
Spatial Distribution.....	26

Branching Ratios	33
Decision Tree.....	35
5. CONCLUSIONS.....	41
REFERENCES	44
VITA.....	48

LIST OF TABLES

Table	Page
1. Missions to Mars.....	6
2. Mars Spacecraft	23
3. Average Nearest Neighbor.....	26
4. Pixel Values for Three Layer Stacks	31
5. Branching Ratio vs. Water and Various Elements.....	34
6. Decision Tree Model Summary (Iteration 1).....	36
7. Decision Tree Risk (Iteration 1)	37
8. Decision Tree Classification (Iteration 1).....	38
9. Decision Tree Model Summary (Iteration 2).....	38
10. Decision Tree Risk (Iteration 2)	40
11. Decision Tree Classification (Iteration 2).....	40

LIST OF FIGURES

Figure	Page
1. Gully Traits (Malin and Edgett 2000).....	2
2. Martian Gullies (Martel 2003).....	2
3. Icelandic Gullies (Martel 2003)	3
4. Water Concentration Map of Mars (Hartman et al. 2003)	3
5. Canals on Mars (Lowell 1906)	5
6. Gully Life Cycle (Hartman et al. 2003).....	11
7. Schematic Morphology of a Martian Outburst Flood Channel (Hoffman 2000)	14
8. Two-dimensional Model Results and Input Datasets (Pelletier 2008)	16
9. Results of MOC Gully Survey (Balme 2006).....	18
10. Cross Sections of the Meridional Water Transport in the Atmosphere of Mars	20
11. Euclidean Distance Between Randomly Created GIS Points.....	27
12. Euclidean Distance Between Low Gullies.....	28
13. Euclidean Distance Between High Gullies.....	28
14. K/Th Global Layer Stack of Water, Chlorine, and K/Th GRS Data	29
15. Si Global Layer Stack of Water, Chlorine, and Silicon GRS Data.....	30
16. Fe Global Layer Stack of Water, Chlorine, and Iron GRS Data.....	30
17. Gullies and Geology	33

18. A Typical MRO Image with the Gullies Digitized.....	34
19. High Gully Branching Ratio vs. Water Concentration	34
20. High Gully Branching Ratio vs. a. Ch Concentration b. K/Th.....	35
21. High Gully Branching Ratio vs. Concentration a. Fe b. Si.....	35
22. Decision Tree (Iteration 1)	37
23. Decision Tree (Iteration 2)	39

ABSTRACT

A SPATIAL ANALYSIS OF GULLIES ON MARS

by

Leon Kincy, B.A., B.S.

Texas State University-San Marcos, Texas

December 2009

SUPERVISING PROFESSOR: NATHAN CURRIT

The purpose of this thesis is to improve the knowledge of Martian gully origins. This study specifically analyzes Martian surface composition, gully structure, and the spatial distribution of gullies. Gully badlands are digitized, and branching ratio vs. various elements composing the surface of Mars, is calculated. The spatial dispersion of gullies is determined to be clustered away from the equator. Few gullies are found within 30° of the equator. Gully sites are overlaid with surface composition data, both elemental and geologic, and findings show the surface of Mars is both a patchwork of minerals and a patchwork of geologic time zones. Evidence is found that indicates gullies

are found in areas high in chlorine and low in water, potassium, iron, and silicon. A decision tree is created to help predict where gullies may occur. Taken together, these findings implicate brine as the likely fluid source for gullies on Mars. Findings also imply the water flow models presented by Clancy (1996) and Kuzmin (2006) may play a role in the formation of Martian gullies.

CHAPTER 1

INTRODUCTION

The possibility of life on Mars has intrigued people for over a century. A necessary requirement for life is water, a substance confirmed to exist on Mars. Malin and Edgett (2000) started a flurry of research on Martian gullies, features typically created by flowing water. Malin and Edgett (2000) observe that although Mars today is a desert planet, numerous geologically young gullies exist. The presence of these gullies on the surface of other features, such as craters, suggests the gullies are young relative to the features on which they lie. Many images, such as those in Figure 1, have been studied and compared to gullies on Earth to try to determine the origin of Martian gullies.

A gully is defined as a surficial feature having an alcove above a channel, and channels are typically associated with water. The gullies in Figures 1 and 2 have inverted triangular shaped alcoves at the head, followed by channels, and triangular aprons at the base, typical of Martian gullies. The gullies in Figure 2A are actually Martian gullies similar in appearance to some terrestrial gullies. The gullies in Figure 2B form badlands (Malin and Edgett 2000). Figure 3 contains three unusual, but not unique, types of Martian gullies. The first image has a small group of gullies with a huge alluvial fan as an apron. The second image has white outcroppings in the vicinity of gullies, and the last

image has gullies lying on dunes. Both white outcroppings and dunes are common on Mars. The map in Figure 4 is a pseudo color image of the distribution of water on Mars detected by the Gamma Ray Spectrometer (GRS). Water is a potential creator of gullies, and the distribution of water in this map may correlate to gully locations. It is important to note that water in this image is unevenly distributed.

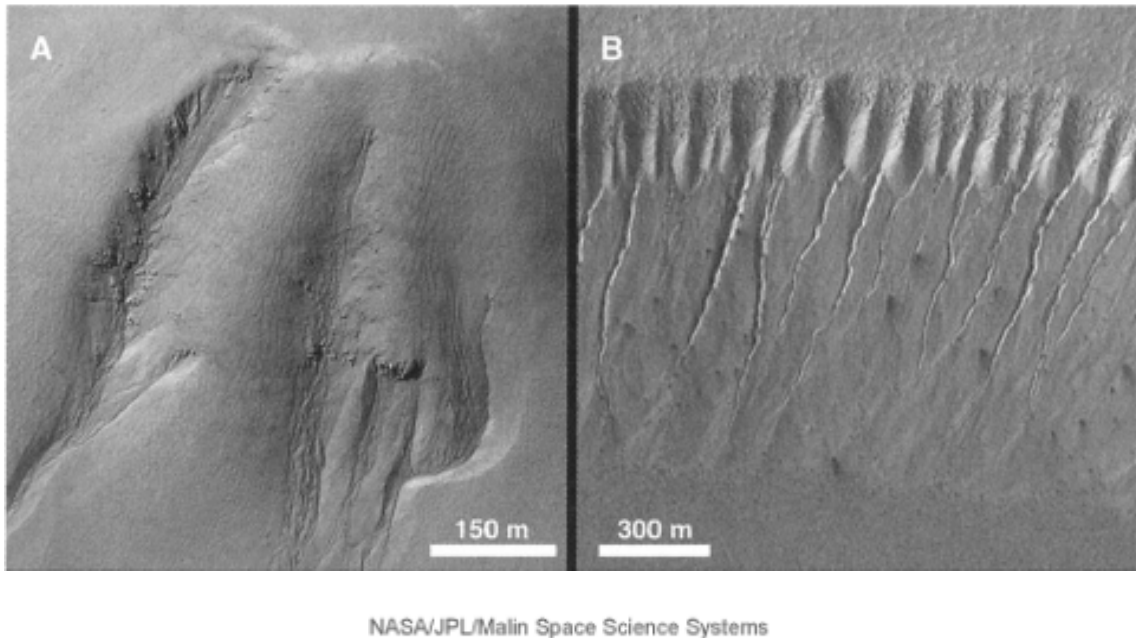


Figure 1. Martian Gully Traits (A) Lengthened alcoves are longer (down slope) than they are wide; (B) where they occur in close proximity, they form badlands (Malin and Edgett 2000, 2330).

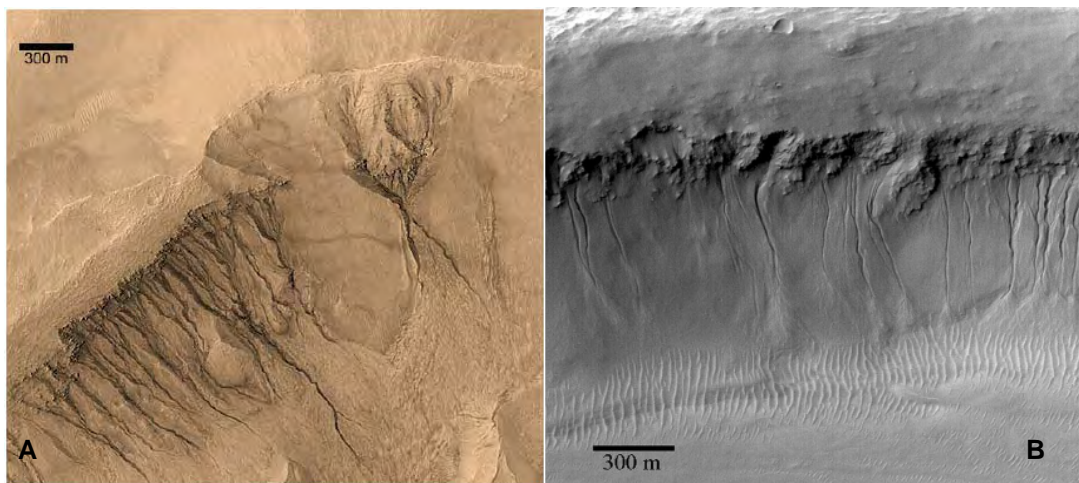


Figure 2. Martian and Earth gully similarities. A. Gullies in a crater captured by the MOC (Martel 2003, 2). B. Icelandic Gullies on a basaltic hillside. (Hartmann 2003, 260)



Figure 3. Unusual Martian gullies. A. A crater gully with a mound of ooze as its alluvial fan. B. White outcroppings and gullies in a crater. C. Gullies on dunes. (ASU 2006)

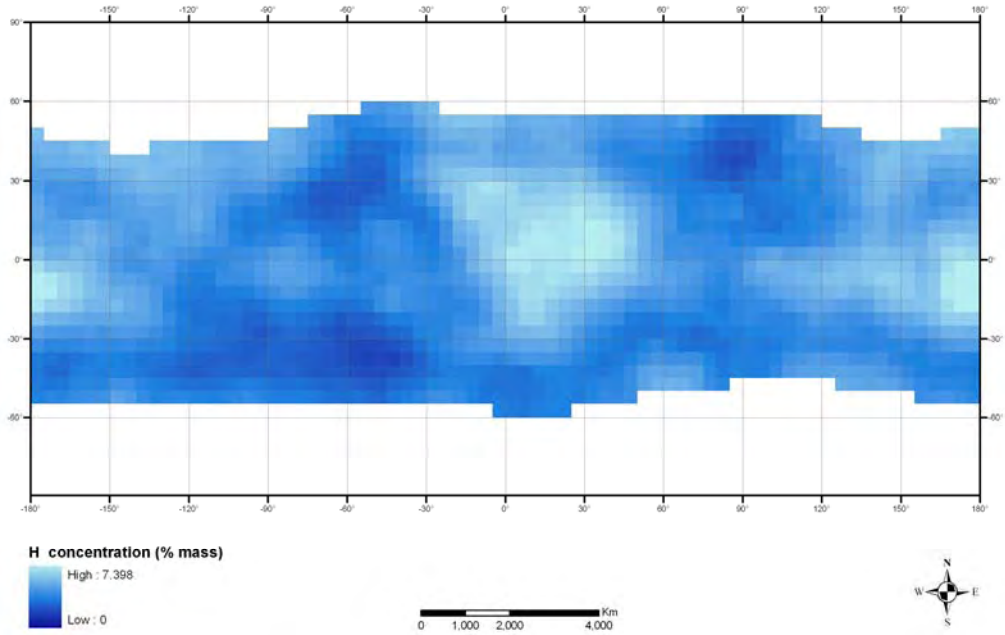


Figure 4. Water concentration map of Mars. Light blue represents a H₂O concentration of 7.4 % vs. soil weight, and dark blue is zero.

Geologic History of Mars

Besides gullies, Mars has numerous volcanoes and river channels that have reshaped its surface (Chapman 2007). None of the volcanoes or rivers is known to be currently active. Mars has three broad geologic time periods: Noachian 4.5 to 3.5 billion years ago; Hesperian 3.5 to 1.8 billion years ago; Amazonian 1.8 billion years ago to the present. These time periods can be divided into dozens of smaller periods. Data about the geologic history of Mars may also correlate to the location of the gullies.

History of Research on Mars

Percival Lowell and Giovanni Schiaparelli conducted early modern research on Mars that received much attention in the media in the late 1800s and early 1900s. They were astronomers who used the most advanced telescopes of the day. Lowell wrote three books on Mars (*Mars*, *Mars And Its Canals*, and *Mars as The Abode of Life*). In the following passage from *Mars And Its Canals*, Lowell describes Schiaparelli discovering canals on Mars,

“But in the course of his work he became aware of hitherto unrecognized ligaments connecting the seas with one another. Instead of displaying a broad unity of face the bright areas appeared to be but groundwork for streaks. The streaks traversed them in all directions, tessellating the continents into a tilework of islands. Such mosaic was not only new, but the fashion of the thing was of a new order or kind. Straits, however, Schiaparelli considered them and gave them the name canali, or channels.” (Lowell 1906, 27).

Figure 5 is a hand drawn map Lowell created in 1894 containing dozens of lines thought then to be canals. Other drawings depict the Martian polar ice caps, clearly visible in telescopes. It is clear in the above passages and drawings in his book, that both Lowell and Schiaparelli believed Mars had evidence of water.

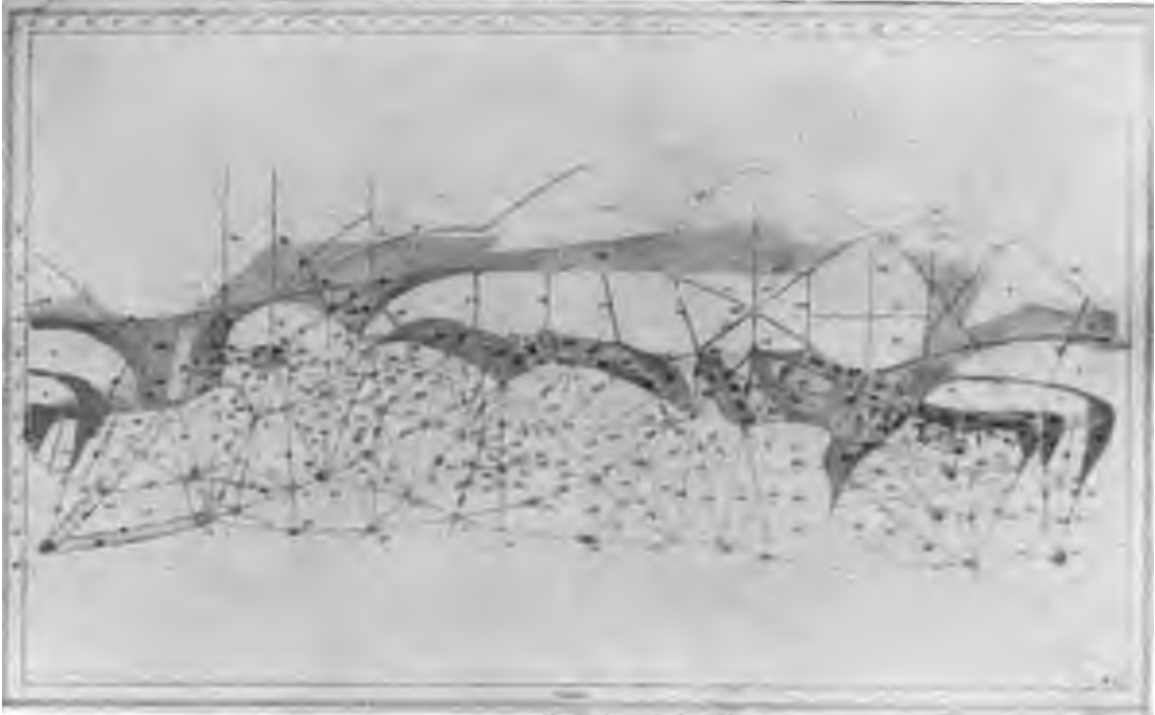


Figure 5. Canals on Mars by Percival Lowell, 1894. (Lowell 1906, 28)

During the periods of World War I and II not much research on Mars was conducted, except for the development of larger telescopes. After the launch of Sputnik in 1957, Mars research took a quantum leap. The Soviet Union, followed by the US and others, sent dozens of unmanned missions to Mars. As seen in Table 1, from 1960 to 2007 a total of 45 flybys, spacecraft, orbiters, landers, and rovers have been launched to Mars, with 18 successful missions. During the 1960s and 1970s, missions to Mars focused on mapping and basic atmospheric measurements (JPL 2009). The US named Viking missions analyzed the Martian soil. In the 1990s NASA continued to chemically analyze the Martian surface with the Pathfinder mission. The success rate of missions has increased in recent years. Table 1 contains all missions to Mars to date.

Table 1. Missions to Mars

Launch Date	Name	Country	Result	Reason
1960	Korabl 4	USSR (flyby)	Failure	Didn't reach Earth orbit
1960	Korabl 5	USSR (flyby)	Failure	Didn't reach Earth orbit
1962	Korabl 11	USSR (flyby)	Failure	Earth orbit only; spacecraft broke apart
1962	Mars 1	USSR (flyby)	Failure	Radio Failed
1962	Korabl 13	USSR (flyby)	Failure	Earth orbit only; spacecraft broke apart
1964	Mariner 3	US (flyby)	Failure	Shroud failed to jettison
1964	Mariner 4	US (flyby)	Success	Returned 21 images
1964	Zond 2	USSR (flyby)	Failure	Radio failed
1969	Mars 1969A	USSR	Failure	Launch vehicle failure
1969	Mars 1969B	USSR	Failure	Launch vehicle failure
1969	Mariner 6	US (flyby)	Success	Returned 75 images
1969	Mariner 7	US (flyby)	Success	Returned 126 images
1971	Mariner 8	US	Failure	Launch failure
1971	Kosmos 419	USSR	Failure	Achieved Earth orbit only
1971	Mars 2 Orbiter/Lander	USSR	Failure	Orbiter arrived, but no useful data and Lander destroyed
1971	Mars 3 Orbiter/Lander	USSR	Success	Orbiter obtained approximately 8 months of data and lander landed safely, but only 20 seconds of data
1971	Mariner 9	US	Success	Returned 7,329 images
1973	Mars 4	USSR	Failure	Flew past Mars
1973	Mars 5	USSR	Success	Returned 60 images; only lasted 9 days
1973	Mars 6 Orbiter/Lander	USSR	Success/Failure	Occultation experiment produced data and Lander failure on descent
1973	Mars 7 Lander	USSR	Failure	Missed planet; now in solar orbit.
1975	Viking 1 Orbiter/Lander	US	Success	Located landing site for Lander and first successful landing on Mars
1975	Viking 2 Orbiter/Lander	US	Success	Returned 16,000 images and extensive atmospheric data and soil experiments
1988	Phobos 1 Orbiter	USSR	Failure	Lost en route to Mars
1988	Phobos 2 Orbiter/Lander	USSR	Failure	Lost near Phobos
1992	Mars Observer	US	Failure	Lost prior to Mars arrival
1996	Mars Global Surveyor	US	Success	More images than all Mars Missions
1996	Mars 96	USSR	Failure	Launch vehicle failure
1996	Mars Pathfinder	US	Success	Technology experiment lasting 5 times longer than warranty
1998	Nozomi	Japan	Failure	No orbit insertion; fuel problems

1998	Mars Climate Orbiter	US	Failure	Lost on arrival
1999	Mars Polar Lander	US	Failure	Lost on arrival
1999	Deep Space 2 Probes (2)	US	Failure	Lost on arrival (carried on Mars Polar Lander)
2001	Mars Odyssey	US	Success	High resolution images of Mars
2003	Mars Express Orbiter/Beagle 2 Lander	ESA	Success / Failure	Orbiter imaging Mars in detail and lander lost on arrival
2003	Mars Exploration Rover - Spirit	US	Success	Operating lifetime of more than 15 times original warranty
2003	Mars Exploration Rover - Opportunity	US	Success	Operating lifetime of more than 15 times original warranty
2005	Mars Reconnaissance Orbiter	US	Success	Returned more than 26 terabits of data (more than all other Mars missions combined)
2007	Phoenix Mars Lander	US	Success	Returned more than 25 gigabits of data

JPL (2009)

Future research on Mars has the goals of determining if life ever arose on Mars, characterizing the climate of Mars, characterizing the geology of Mars, and preparing for human exploration of Mars. In the near future NASA may send scout missions composed of airplanes or balloons, sample return missions, a deep drill lander, and a biological field laboratory JPL (2009).

To date, these missions have shown that many Martian geomorphic features are similar to features found on Earth. What is not known is whether or not the same processes that create Earth's geomorphic features are also responsible for creating Martian geomorphic features. On Earth, various fluids play a role in the creation of gullies. Therefore, the purpose of this study is to improve upon the knowledge of the fluid source of Martian gullies. Water is one possible source, and is needed for both

indigenous life, and for human exploration. Knowing the attributes of both gullies and badlands has the potential to indicate the fluid source of the gullies.

CHAPTER 2

LITERATURE REVIEW

The literature about gullies on Mars focuses on eight primary topics: gully formation, fluid sources, Martian obliquity (planetary tilt), Martian surface composition, gully orientation, gully structure, atmospheric and water cycles, and spatial distribution. Some literature is exclusive to Mars, and some offers Earth-Mars comparisons. A review of each of these topics is necessary to understand the origin of gullies. Therefore, I review these concepts to structure the basis for my study of Martian gullies.

Gully Formation

On Earth, extensive gully studies reveal that gullies typically form on barren slopes; this is relevant to Mars since Mars has no known vegetation to hold soil in place. Malin and Edgett (2000) state the Martian gullies resemble terrestrial gullies, and are formed by sapping (seeps and springs) and debris flows (Malin and Edgett 2000, 2333). Hyde et al. (2007) use remotely sensed data to create a burn severity distribution index (BSDI) for a Montana forest fire. They counted the quantities of gullies for several sectors of the fire area. They conclude gullies on Earth form at or near the tops of barren slopes, and never at the bottom of slopes. Gabet and Bookter (2008) conducted a ground survey of gullies after another Montana forest fire. They found channelization on fire

scoured slopes, but not on otherwise similar vegetated slopes. Furthermore Gabet and Bookter conclude that the widths and depths of gullies increase downslope, and the volume of gully debris flows increases exponentially with drainage area. Rijsdijk et al. (2007) conducted a field survey of a humid agricultural region of Indonesia, including measuring sediment volumes, and rainfall runoff. The area has had erosion problems due in part to both farming practices and poorly built roads and trails. They calculated runoff coefficients (percentage of rainfall not absorbed by the ground), and the highest runoff coefficients were associated with the largest proportion of impervious surface within the subcatchment (Rijsdijk et al. 2007, 48).

Gully Fluid Sources and Obliquity

Martel (2003) systematically identifies and describes all hypothesized origins of gullies on Mars. These origins include water seepage, snowmelt, seepage of brines, outbursts of CO₂, geothermal activity, or dry flows of windblown dust and silt. Each of these topics is reviewed below.

The water seepage hypothesis is that water drains out of the sides of hills and craters and creates gullies as on Earth. Hartmann et al. (2003) compares images of Martian gullies with images of Icelandic gullies, taken in the field. They propose a 4 stage life cycle for Martian and Icelandic gullies, shown in Figure 6. The main obstacle to acceptance of this hypothesis is that water is unlikely to be liquid so close to the surface of Mars where the current temperature and pressure only allows liquid water to exist for brief periods. A possible answer is the wide ranging obliquity (planetary tilt) cycle of Mars—up to 48° (Touma and Wisdom 1993, 1294). They measured the secular spin orbit resonance (wobbling) of Mars over the past 80 million years. With the planet being

heavily tilted, the polar regions receive more direct sunlight and thus experience higher temperatures. Touma and Wisdom (1993) conclude that about 4 million years ago the obliquity of Mars changed from of approximately 28° – 48° to its current range of 15° - 35° . These findings mean that the Martian poles are colder now than they used to be, and water may have been near the surface in previous geologic periods.

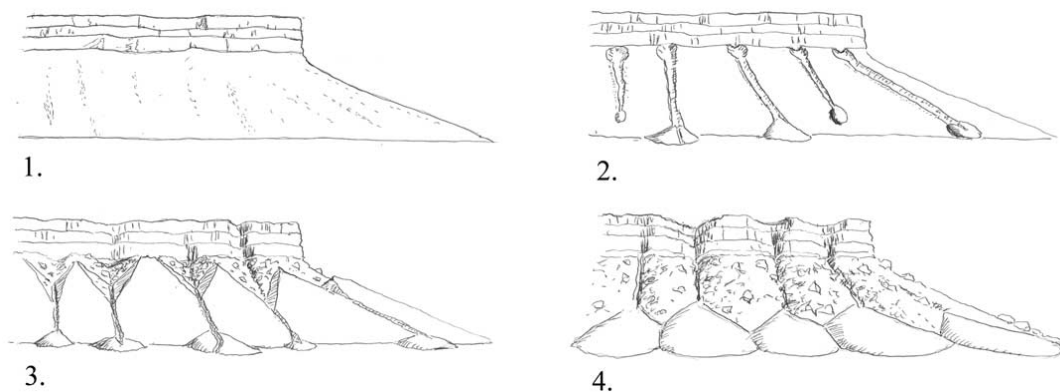


Figure 6. Gully Life Cycle. Schematic cartoon showing four stages of evolutionary development. Stage 1 shows a talus slope with no gullies, but minor albedo features created by downslope movements. This is typical of low-latitude Martian slopes. Stage 2 shows gully formation, usually starting near the talus/ outcrop interface and ending either partway downhill or in debris fans. Stage 3 shows further development of the upper end of the gullies, eroding the talus and carving it into triangular wedges pointing uphill, with facets of the original talus still exposed. Stage 4 shows late development characterized by deeper uphill alcoves, removal of the original talus, and/or coalescing debris fans. (Hartman et al. 2003, 265)

Similarly, Bryson et al. (2008) studied the possible life span of ice on Mars. They ground pieces of terrestrial basalt and sieved to the selected grain sizes: <63 , 63 – 125 , and 125 – 250 μm . The fine-grained basalt was then baked overnight at 110° C and sealed to limit adsorption. The sample was then cooled in a sealed chamber at -20° C. Pure water was frozen in a beaker with a thermocouple placed on the surface. This was covered with layers of basalt 2.5 to 50 mm deep. The chamber was opened and then allowed to warm. The amount of ice remaining was measured at regular intervals. The study concluded ice 1m thick below 1m thick soil can exist for at least 600 years, and at lower depths ice can

exist for up to 400,000 years—the time of the last large obliquity change (Bryson et al. 2008, 454).

The snow melt hypothesis is that snow melts down the slopes of craters and hills during periods of high obliquity. This hypothesis is bolstered by the fact that snow is known to exist on the slopes of craters and hills. Christensen (2003) proposes a detailed model for snow melting at the poles during high obliquity, transport and resnow deposition in mid-latitudes, and finally remelting and gully formation during low obliquity. Furthermore melting and gully formation could currently be occurring in mid-latitudes (Christensen 2003, 45). Lee et al. (2001) studied gullies formed by snowmelt on Devon Island, Canada. The gullies are located at a research site in northern Canada, and some of the gullies are located inside the Haughton impact crater (meteor). The site is chosen for its cold climate and crater, an environment possibly resembling Mars.

The brine hypothesis resembles the water seepage hypothesis, except that brine, a solution of salts dissolved in water, drains out of the ground instead of water. This hypothesis has an advantage over the water seepage hypothesis: Brines have lower freezing points, and are thus more likely to exist as liquids at low temperatures. Brines are the last liquids to freeze and the last to melt (in aquifers). Furthermore Nakhlite meteorites believed to be from Mars (based upon Viking mission results) show exposure to salts containing chlorine, iron, and silica (SiO_2) (Bridges and Grady 1999). Rao (2005) also studied Nakhlite meteorites and Pathfinder images, and found evidence of Cl and Br salts in both. Andersen et al. (2002) studied cold springs on Canada's Axel Heiberg Island, where the climate resembles that of Mars, and where the mean average air temperature is -15°C , and the brine temperature is 6°C . They found springs on the island

and resulting salt pans, but no such features have been observed on Mars (Andersen et al. 2002, 6). Jagoutz (2006) examined images taken by NASA's Spirit and Sojourner rovers, compared them to terrestrial images, and concluded that salt fragmentation of rocks occurred. These studies provide evidence that suggest the brine hypothesis may previously have been important on Mars.

The CO₂ hypothesis is that CO₂ liquid bursts out of aquifers. CO₂ can exist in liquid state at current Mars surface temperature and pressure, at least part of the year. Musselwhite et al. (2008) propose a model for gully formation caused by CO₂, and note that CO₂ specifically exists on Mars as both a gas and solid. In this model underground dry ice thaws in the summer, and pyroclastically explodes (Musselwhite 2008, 1284). Hoffman (2000) also proposes a CO₂ model, but one that is less explosive, more like an avalanche. In this model liquid CO₂ and CO₂ vapor create a decompression front that slide debris sheets down a slope. He describes such events a cryoclastic (Hoffman 2000, 3330). The Hoffman model can be seen in Figure 7. Ishii et al. (2006) overlaid locations of CO₂ seasonal deposits with locations of imaged gullies, and found correlations. The presence of this CO₂ implies gully formation via avalanches (Ishii et al. 2006, 1647).

The geothermal activity hypothesis does not provide a liquid source, but rather a heat source to melt ice or snow. Mars has many volcanoes (although none are known to be currently active). Hartmann (2001) compared physical traits of gullies in Iceland to gullies on Mars, and created a theoretical model where underground geothermal heating melts water ice located in aquifers (Hartmann 2001, 409). Mellon and Phillips (2001) examined Mars obliquity, and gully slope angles. They concluded the increase in surface temperature due to high obliquity is not enough to melt ice. However nominal geothermal

heating a few hundred meters underground would be sufficient to melt ice (Mellon and Phillips 2001, 23172).

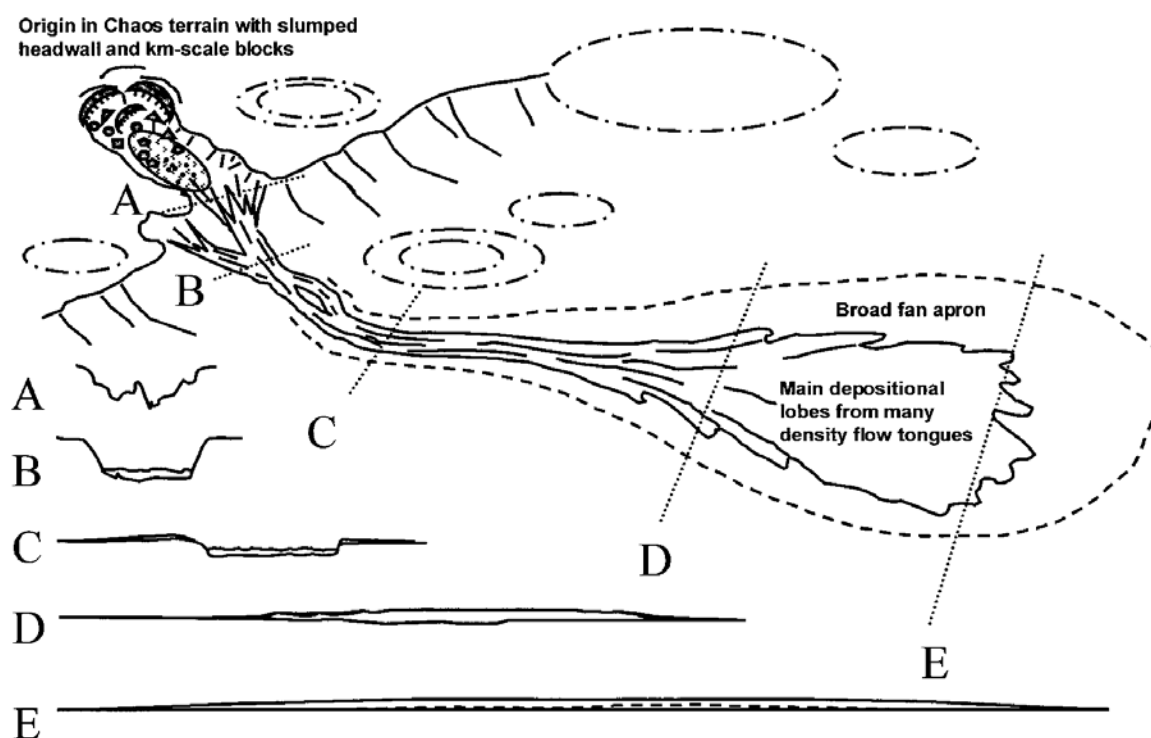


Figure 7. Schematic morphology of a Martian outburst flood channel. Flow originates from a collapsed zone of kilometer-scale slumped, rotated, and slipped blocks at an area of significant topographic relief (1–5 km over short lateral distances). Rather than generating a conventional avalanche or debris flow deposit, the pressurized volatiles within the kilometer-deep layered regolith outgas abundant volumes of CO₂, fragmenting the host rock and converting it into a dense cloud of debris lubricated by gas. The flow proceeds downslope, rapidly amalgamating from a series of V-shaped ravines or chutes and scouring a broad shallow channel and possessing enough momentum to spill over “minor” topographic obstacles (up to several hundred meters in elevation). Characteristic features include teardrop-shaped islands and parallel lineations in the channel floor (caused by second-order linear rolls within the flow). Adjacent terrain may be coated by air fall deposits and overspill flow lobes. In the terminus of the flow—the northern lowlands—the flow spreads out into a low-relief depositional sheet. Since density flows are bottom-seeking, any topographic lows are preferentially filled in. The net result is an exceedingly flat and smooth depositional surface, with a gentle gradient northward—an equilibrium profile for these low-friction flows. Scale: A–B, 5 to 50 km long, 1 to 50 km wide; B–D, 100 to 2000 km length, 10 to 250 km width; D–E, up to another 1000 km long and wide. (Hoffman 2000, 334)

Lastly, dry flows exist on Earth, produce features similar to gullies, and are similar to avalanches. Figure 8 contains some of the results of Pelletier et al. (2008). They examined High Resolution Imaging Science Experiment (HiRISE) images for erosion and deposition, and in particular the width and depth of gullies in each portion (alcove, channel, and apron) of the gully. They conclude the images examined likely have a dry source (Pelletier 2008, 214).

Martian Surface Composition

Many studies have focused on the chemical data obtained from the Gamma Ray Spectrometer (GRS). Boynton et al. (2007) created several maps for all of the elements detected by GRS. These maps are global and have a $5^\circ \times 5^\circ$ (longitude-latitude) resolution. Both Taylor et al. (2006a) and Taylor et al. (2006b) report GRS data showing concentrations of all GRS elements that vary amongst geologic regions. Taylor et al. (2006a) even specify areas of high water concentration. Hahn et al. (2007) produced a Martian geologic map of the three major time periods mentioned in Chapter 1. Frey et al. (2004) use both MOC and (GRS) data to correlate detected hydrogen with the depths of known gullies. A planet wide map was created showing the location of hydrogen throughout the planet. The authors found the gully root depths in hydrogen rich areas begin relatively closer to the surface, whereas gullies in hydrogen poor areas start further below the surface. Also, in less hydrogen rich areas, the overall range of depths at which gullies form is significantly larger (Frey et al. 2004, 1977).

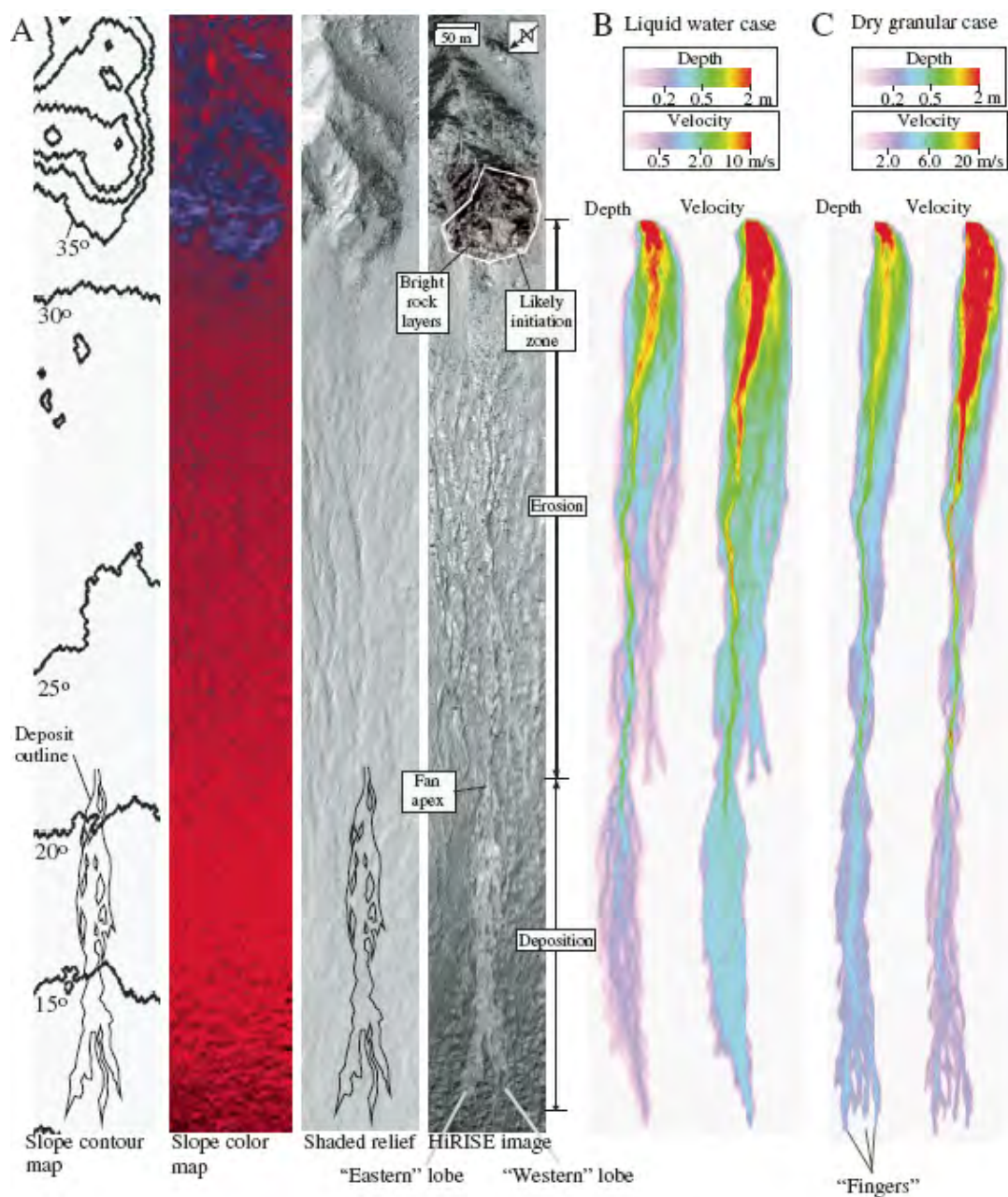


Figure 8. Two-dimensional model results and input datasets. A: Slope contour map, slope color map, shaded relief map, and portion of High Resolution Imaging Science Experiment (HiRISE) image (PSP_001714_1415) of initiation and runout zone of bright gully deposit in Centauri Montes region discovered by Malin et al. (2006) (see footnote 1). The slope map was spatially averaged before contouring to minimize microtopographic variability. B: Color maps of peak depth and velocity for the best-fit liquid water case with fluid-loss rate of 0.77 mm/s. C: Color maps of peak depth and velocity for dry granular case. (Pelletier et al. 2008, 212)

Gully Orientation

Several papers study the direction in which whole gullies or badlands face. Malin and Edgett (2000) were the first to notice an apparent correlation between gully presence and gully orientation. This study observed the following geographic relations:

1. About one third of gullies lie within impact craters, one quarter lie within pits in the south polar region, and one fifth lie within two river valleys.
2. About 50% are south facing and 20% north facing.
3. About 70% pole facing rather than equator facing.
4. About 90% occur south of the equator.

(Malin and Edgett 2000, 2330).

Heldmann and Mellon (2004a) examined 100 southern hemisphere Martian gullies, and found more than 75% face south. Mohan and Bridges (2004) selected gullies using both MOC and Mars Odyssey Thermal Imaging Emission Systems (THEMIS) data, and found longer steeper gullies have a slight preference for facing poleward (south) (Mohan and Bridges 2004, 1339). Balme et al. (2006) also evaluate the lateral orientation of the gullies, using pseudo circular diagrams to depict the north-south orientation of gullies by latitude. The data used include both MOC and Mars Express High Resolution Stereo Camera (HRSC). The paper concludes that most gullies lie between -30° and 50° latitudes, and usually face a pole (Balme et al. 2006, 1). Figure 9 contains some of the pseudo circular diagrams and histograms of gully latitudinal distribution from Balme et al. (2006). The gullies are divided into 4 categories: crater walls, valley walls, knob hills, and pit walls. The most common gully group, crater walls, has gullies typically facing south. This is significant, because as circular shaped features, craters potentially can

have gullies facing in any direction.

Lanza and Gilmore (2006) describe the depths, north-south orientation, and slope angles of over 160 gullies. They used DEMs to create regions containing the gullies, using data from the Mars Orbital Altimeter (also on board the Mars Global Surveyor spacecraft). Next the DEMs were overlaid with MOC photos, within Geographic Information System (GIS) software. Next the gullies were digitized. Finally depth and slope were extracted from the DEMs (Lanza and Gilmore 2006, 1). The resulting data show north-south orientations similar to Malin and Edgett (2001, 2330). The average depth of a gully is 202 m, and the average slope angle is 17.4° (Lanza and Gilmore 2006, 1-2). They conclude that a combination of orientation, slope, and depth are needed to provide the conditions to form gullies (Lanza and Gilmore 2006, 2). Heldmann and Mellon (2004a) also examine gully alcoves, using Mars Global Surveyor Thermal Emission Spectrometer (TES) data, and MOLA data. (TES is an IR only instrument). They determined alcove depths range from 200m to 700m.

Atmospheric and Water Cycles

Clancy et al. (1996) proposed a cycle where water in the Martian equatorial soil condenses into the atmosphere and is transported to the polar regions. This cycle was expanded upon by Kuzmin et al. (2006). In particular the saturation altitude of water, in the atmosphere, is almost twice as high at perihelion (closest distance to the sun), and later during aphelion (furthest distance away from sun), vapor becomes saturated at lower heights and the bulk of the atmospheric water mass is captured in the near-equatorial cloudy belt and, thus, is only weakly transferred to the southern hemisphere. Furthermore

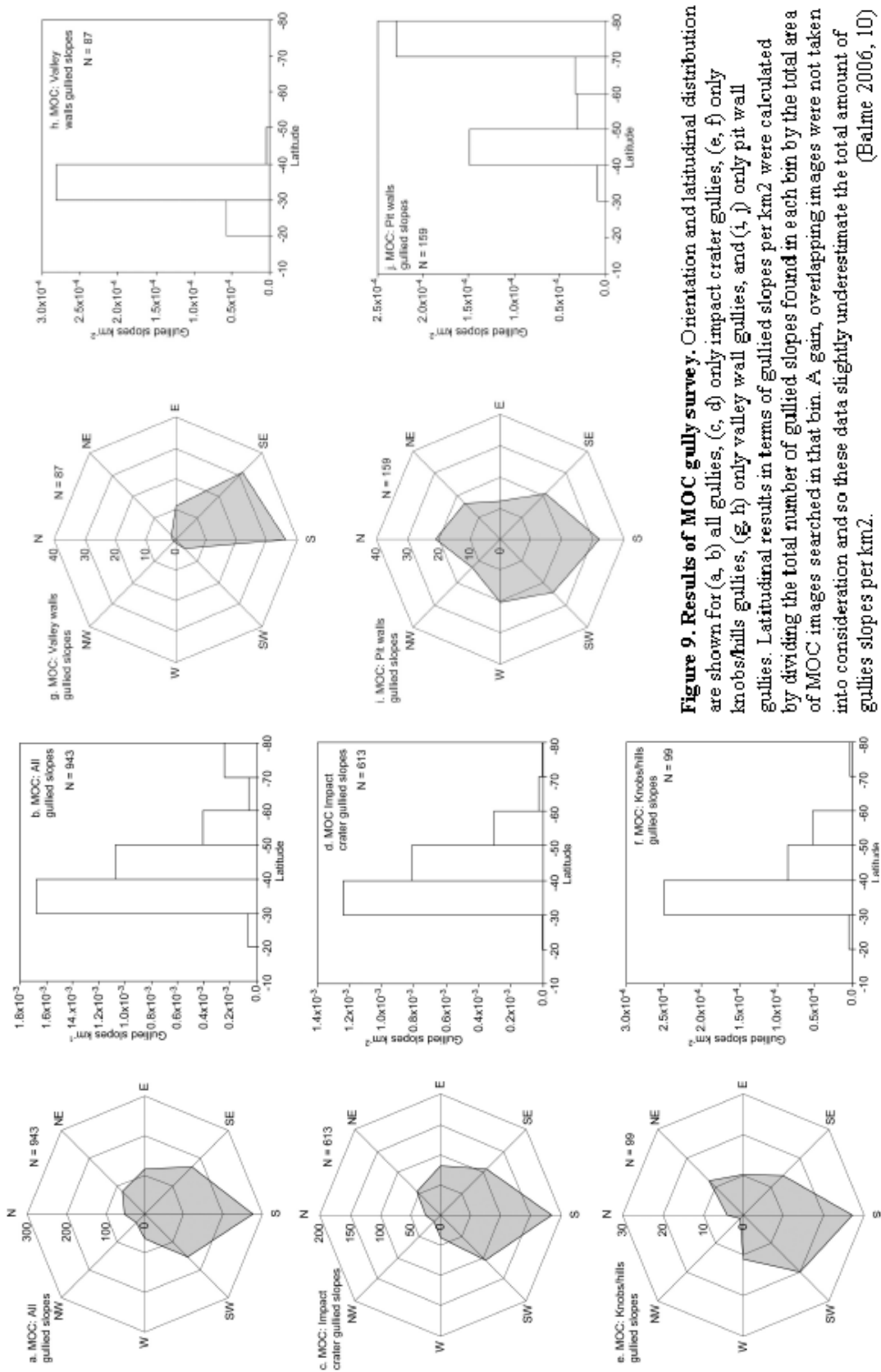


Figure 9. Results of MOC gully survey. Orientation and latitudinal distribution are shown for (a, b) all gullies, (c, d) only impact crater gullies, (e, f) only knobshills gullies, (g, h) only valley wall gullies, and (i, j) only pit wall gullies. Latitudinal results in terms of gullied slopes per km² were calculated by dividing the total number of gullied slopes found in each bin by the total area of MOC images searched in that bin. A gain, overlapping images were not taken into consideration and so these data slightly underestimate the total amount of gullied slopes per km². (Balme 2006, 10)

some of this water may freeze out and hydrate minerals in the Martian soil (Kuzmin 2006, 97-100). Figure 10 depicts this cycle.

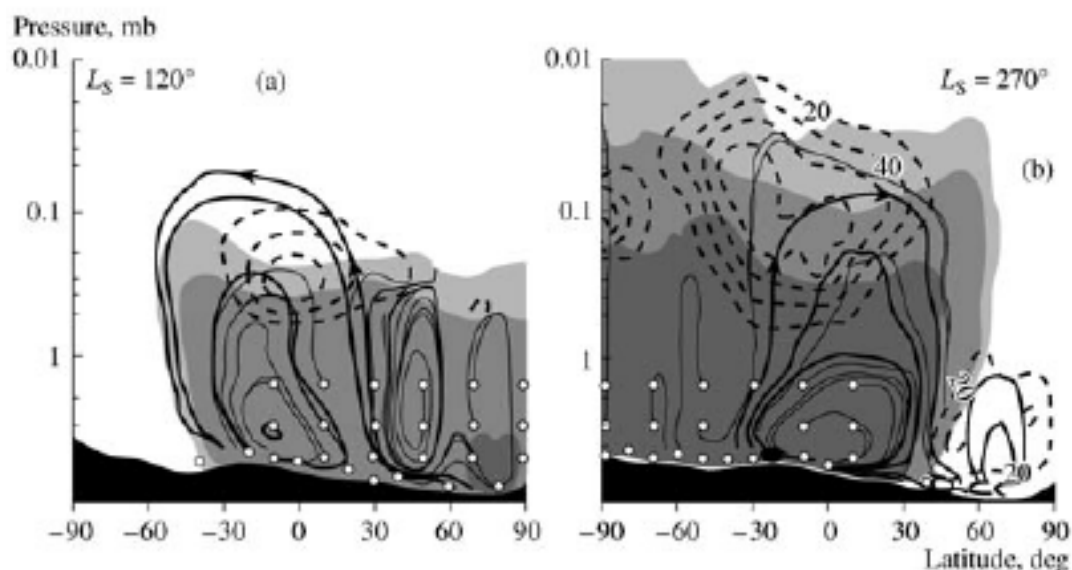


Figure 10. Cross sections of the meridional water transport in the atmosphere of Mars at (a) aphelion (northern summer) and (b) perihelion (southern summer) constructed by numerical simulations in (Rodin and Wilson 2006). The regions where water vapor is present in the Martian atmosphere are colored gray; the solid thick lines show the stream lines of the Hadley circulation cell; the thick arrows indicate the direction of the air mass displacement; and the thin lines show the meridional water advection in the Martian atmosphere according to the results of the atmospheric general circulation model taking into account phase transformations and cloud formation. The thick dashed lines show the localization of ice clouds, the corresponding cloud ice content is given in ppmv; and small circles schematically represent the sources of water vapor. (Kuzmin 2006, 98)

Spatial Distribution

Several studies have cataloged gully locations in order to find spatial patterns. Heldmann and Mellon (2004a) found that the number of gully systems, in the southern hemisphere of Mars, steadily declines as one moves poleward of 30°S, reaches a minimum value between 60°- 63°S, and then again rises south of 63°S. Heldmann et al. (2007) examined 137 northern hemisphere gullies in MOC images, and found most are located between 30° and 55° latitude. Bridges and Lackner (2006) also examined 72

northern hemisphere gullies contained in MOC images and also found most northern gullies lie between 30° and 55° latitude.

Objective

While there is no consensus as to the origin of all Martian gullies, the topics of study reviewed in this chapter comprise the primary theories of Martian gully formation. From this review of Martian gullies and their likely causes arise certain factors that are not well understood or have not been fully investigated. The most glaring gap in knowledge about Martian gullies is whether or not the same processes that create Earth's geomorphic features are also responsible for creating Martian geomorphic features. The objective of this research is to examine Martian gullies and determine if they exhibit spatial and statistical relationships to geologic and elemental Martian features that may indicate the underlying cause of gully formation on Mars.

Of the eight topics of study reviewed in this chapter, this study specifically analyzes Martian surface composition, gully structure, and the spatial distribution of gullies. This research statistically examines: (1) patterns of gully distribution and (2) measures of, and relationships between, gully structure and elements using linear regression and a non-parametric decision tree classifier. Performing these analyses will provide a clearer view of Martian gullies and elucidate possible origins of those gullies. The research will provide additional evidence supporting existing theories of the sources of Martian gullies.

CHAPTER 3

DATA AND METHODS

Study Area

The whole planet of Mars will be used as a study area. Gullies on Mars are typically located in meteor craters, in mid-latitudes from 60° N to 60° S. Furthermore geologically older areas serve as gully sites. Mars is the fourth planet in our solar system, and every 22 months is in closest proximity to Earth. In the past two decades NASA and other international space agencies typically have sent missions to Mars every 22 months. The Gamma Ray Spectrometer (GRS) collected elemental data from 50° N to 50° S. Therefore only gullies in this latitudinal range will be analyzed.

Data Collection

NASA has collected remote sensing data on Mars for decades. The data for this study have been collected using several NASA instruments, as shown in Table 2. Mars Global Surveyor (MGS) spacecraft's visible band Mars Orbital Camera (MOC), the MGS infrared Thermal Emission Spectrometer (TES), Mars Odyssey's visible-IR Thermal Emission Imaging System (THEMIS), and Mars Reconnaissance Orbiter (MRO) spacecraft's High Resolution Imaging Science Experiment (HiRISE) all provided images. Odyssey's Gamma Ray Spectrometer (GRS) provided substance data. MRO HiRISE

is the source for most of the images used in this research. Thirty three images are selected from nearly 500 images identified as having gullies by the HiRISE archivists. These 33

spacecraft	start of mission	products	instruments	resolution
Viking A	19-Jun-76	geologic base maps		300 m
Viking B	7-Aug-76	geologic base maps		300 m
MGS	11-Sep-97	images	MOC	1.5m
Odyssey	24-Oct-01	images	THEMIS	100m
		elemental data	GRS	5° x 5°
MRO	10-Mar-06	images	HiRISE	0.3m

images are selected because of their clarity and the high level of gully branching. An additional 33 images with gullies are chosen randomly. Using GIS, 33 randomly located points are created for the study area as an experimental control. The 33 high branching MRO images are processed using the USGS pds2world Perl script. This script, requires only one command, and gives MRO images the proper projection.

Data Limitations and Assumptions

Data limitations include (1) the low resolution of some of the satellite sensors used to image Mars. The GRS resolution is especially coarse—only 5° longitude x 5° latitude. Although all the instruments are of high quality, there is no substitution for direct data collection. Most, but not all, of Mars has been imaged. It is assumed the gullies that have been imaged actually are gullies and are a reasonable representation of all gullies.

Preprocessing and Information Extraction

The 33 high gully images are imported into remote sensing software, and gully badlands are digitized, and exported into vector files. These vector files are then converted into shapefiles using GIS software, and gully branching ratios are calculated. The average number of branches from each gully in a badland is then calculated. A branch total is calculated by following a route, starting at the bottom of a gully, and moving up. Each time a branch is found, the branch total is increased. Most gullies have multiple routes. The route with the most branches is used to calculate the branching ratio.

The shapefiles and images are mapped using GIS software. Other layers, such as Hydrogen concentration, geologic age zones (geologic time periods), and elevation, are obtained and mapped. Thirty three additional images identified as having gullies, by the archivists of the MRO images, are randomly selected and mapped using the xy coordinates given on the HiRise web site.

Gully images, gully shapefiles, and elements data are loaded into GIS. The values of five elemental layers (H, Cl, Fe, Si, and K/Th) and more than 95 geologic formations are overlaid and spatially joined to the center point of all 66 images and 33 random GIS points. Each point identifies the location of high branching, low branching, or randomly placed points. Color image composites are created to display elemental concentrations on Mars. These images are then imported into GIS and overlaid with gully layers, so the pixel values for each gully can be determined. Water and chlorine are used in each layer stack, because water is in all proposed gully formation hypotheses, except CO₂ and dry flow is the principle fluid component.

Statistical Methods

Average Nearest Neighbor Analysis and Euclidean Distance are used to determine the spatial dispersion of the high gullies, the low gullies, and the random GIS points. Linear regression between elements and branching ratios are calculated using statistical software. Finally, a decision tree is a non-parametric technique used to determine rules for distinguishing gullies from non-gully sites where the elemental, geologic, and spatial data are independent variables. A decision tree creates a series of nested rules based on the elemental and geologic data that, when applied, predict whether a particular point is found at a gully location or not. The rules are determined by separating the 99 points into training and test sets. The rules are iteratively created on the training set and statistical accuracy is calculated on the test set so as to avoid overtraining. Once the greatest accuracy is obtained on the test set, the rules are set and the decision tree algorithm terminates.

Two sets of iterations of decision tree are run. The first set includes high gullies as a dependent variable target. Parameters include water, Ch, Fe, Si, K/Th, and geology as independent variables, and both training and test components. The minimum parent node size is set to two and the minimum child node size is set to one. In both iterations only the training and test proportions are changed. The training percentage is changed in 10% increments from 90% to 0%, and also for the test sample. The second set of iterations used the same high gully target, and the same independent variables, but also included longitude and latitude as dependent variables. This inclusion of additional independent variables can lead to the creation of different decision tree nodes and can result in different variables being predictors.

CHAPTER 4

RESULTS

Spatial Distribution

Average Nearest Neighbor analysis is performed to determine if the spatial distribution of Martian gullies is clustered, dispersed, or random. A nearest neighbor ratio (NNR) equal to one indicates randomness; a NNR less than one indicates clustering, and a NNR greater than one indicates dispersion. Table 3 shows the results of the Average Nearest Neighbor test. As expected the randomly created GIS points have a NNR close to 1.0. The high gullies have a NNR of 0.47 and the low gullies have a NNR of 0.85, indicating that they are clustered spatially.

type	Observed Mean Distance	Expected Mean Distance	Nearest Neighbor ratio	Z score
random	17.82	16.09	1.11	1.18
low	12.85	15.15	0.85	-1.67
high	7.49	15.79	0.47	-5.78

Figures 11-13 are the results of the ArcMap Euclidean Distance procedure. White areas in Figures 11-13 are unsampled areas (i.e., greater than 50 degrees from the equator). With the exception of K/Th, GRS data are only available for the center 110° latitudes. In Figure 11, only four yellow ellipses (approximately 10 decimal degrees in

diameter) contain two or three points, and the map has little shades of magenta and blue—locations far from a point (up to 60 dd in diameter). In contrast, a majority of the low and high gullies appear within yellow ellipses. More significantly, all of the high gullies appear in only four orange zones, and the map contains more magenta and blue. These maps show that the randomly placed points really are randomly placed, and suggest that the actual locations of gullies are clustered.

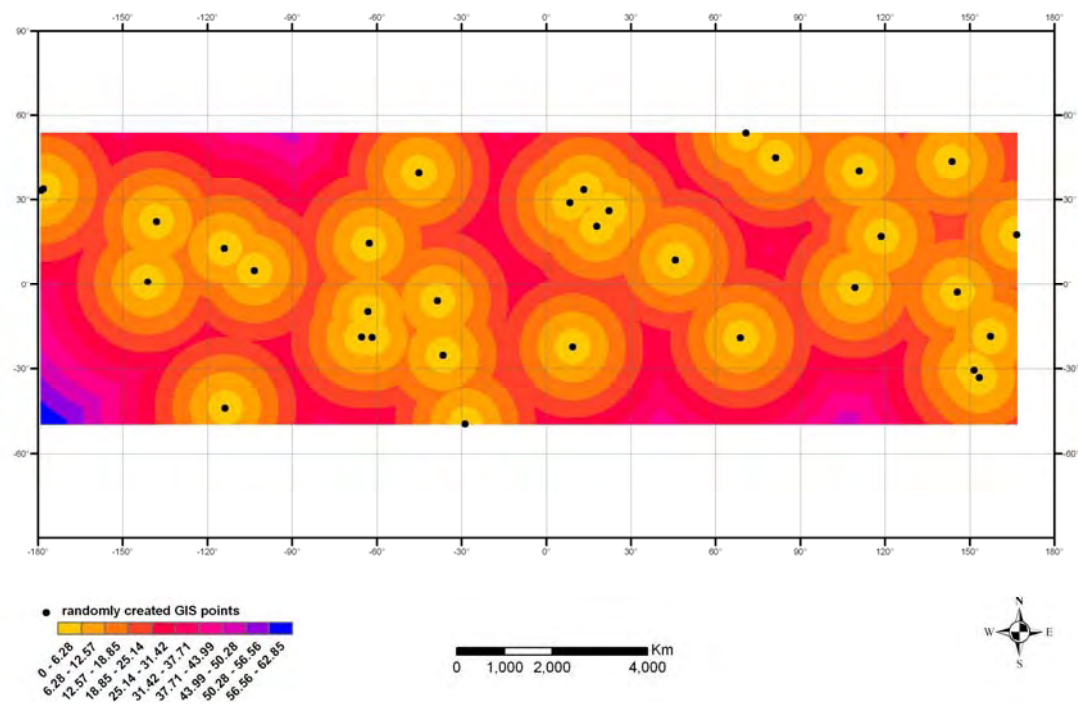


Figure 11. Euclidean distance between randomly created GIS points.

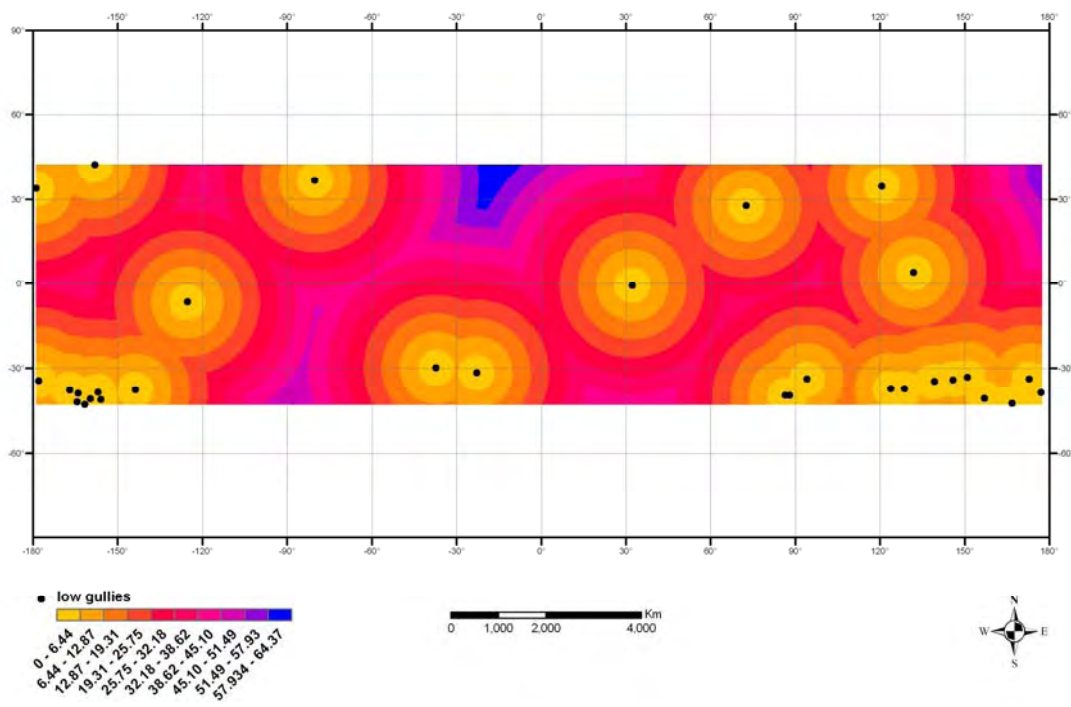


Figure 12. Euclidean distance between low gullies.

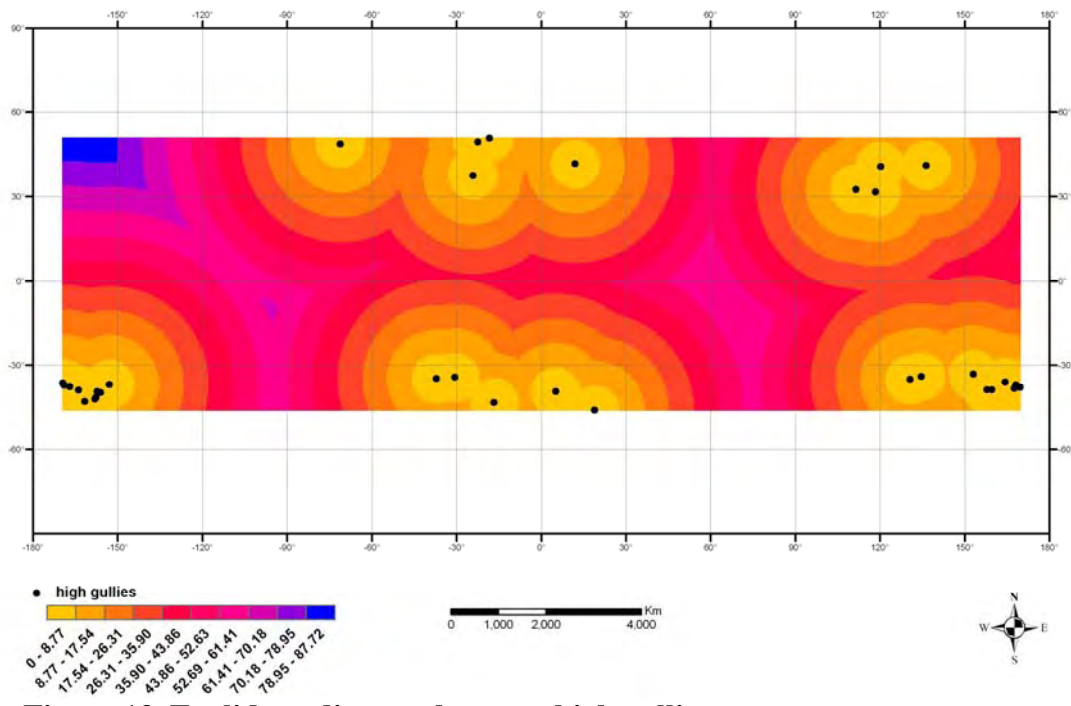


Figure 13. Euclidean distance between high gullies.

The map in Figure 14 is prepared using Cl, water, and K/Th as the RGB bands, respectively. The map in Figure 15 is prepared using Cl, water, and Si, and the map in Figure 16 is prepared using Cl, water and Fe. The global color pattern in Figure 14 is greener (indicating the dominance of water) and redder (indicating the dominance of Cl) than the colors in Figures 15 and 16, with isolated cyan and blue patches. In Figure 14, 27 out of 33 gullies appear in areas of shades of orange, indicating areas with higher concentrations of chlorine relative to the concentration of water, and even lower concentration of K/Th. A bright orange implies higher levels of both chlorine and water relative to a dark orange. In both Figures 15 and 16, the 31 out of 33 high branching gullies appear in areas of magenta, indicating the presence of chlorine, and similarly high levels of silicon and iron. Water levels are relatively low.

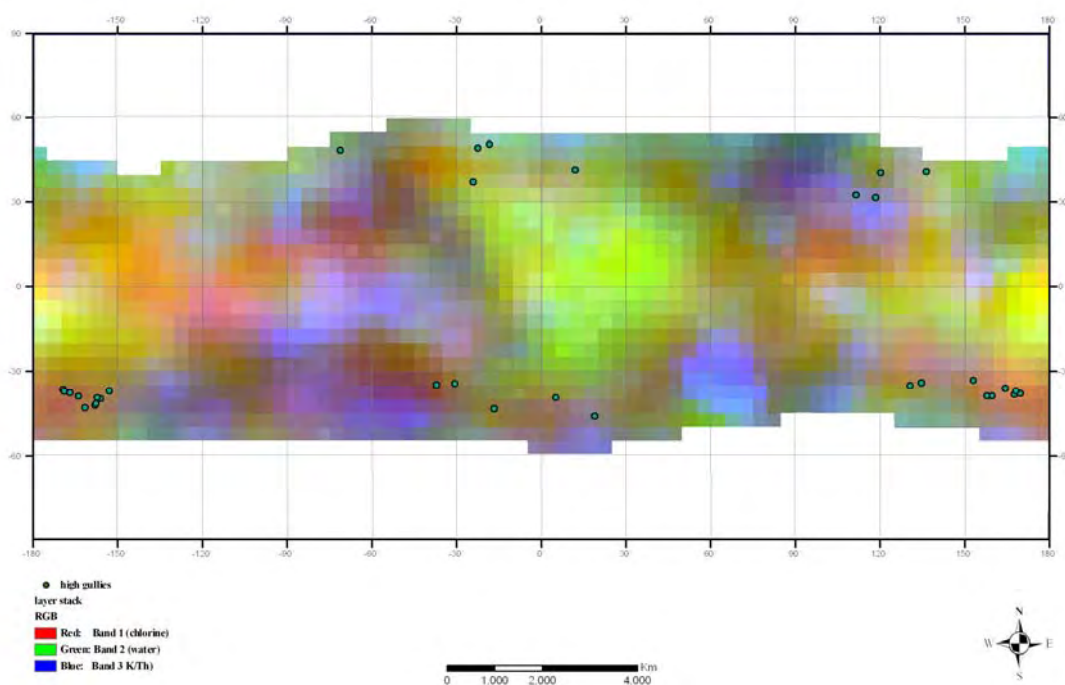


Figure 14. K/TH Global layer stack. Water, chlorine, and K/Th GRS data, with high gully locations.

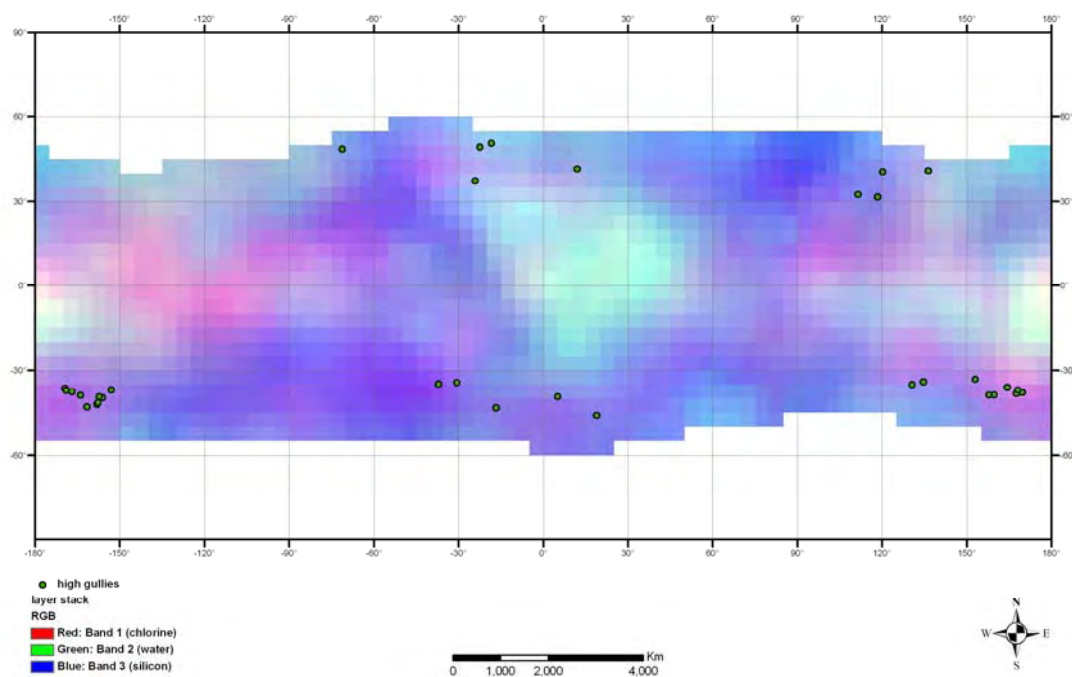


Figure 15. Si Global layer stack. Water, chlorine, and silicon GRS data, with high gully locations.

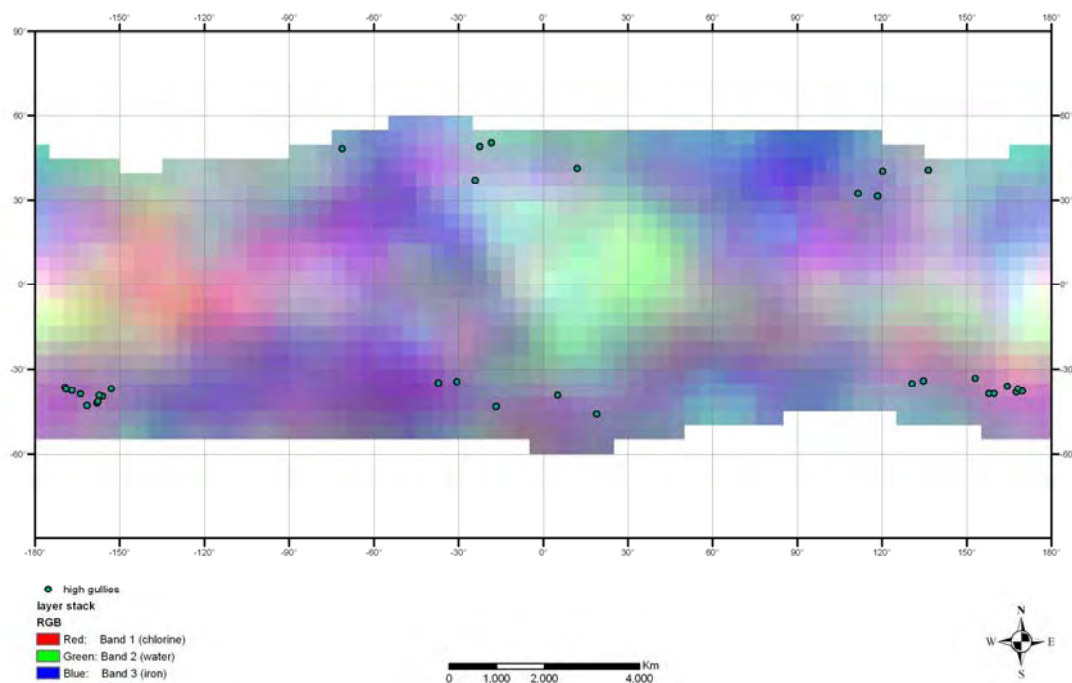


Figure 16. Fe Global layer stack. Water, chlorine, and iron GRS data, with high gully locations.

These color difference can be examined quantitatively using the 8-bit gray scale (0-255) value for every pixel where a gully is located. Table 4 contains these values, where 0 indicates a complete lack of the element, and 255 is the maximum presence of the element. The gullies are grouped into five zones: southwest (sw), south central (sc), southeast (se), north central (nc), and northeast (ne). In the blue column for the K/Th layer, in the three southern zones, the values are, all but twice, below 100. In the south, for all three layer stacks, red values are always greater than green values, which are all but once greater than blue values. In the north, RGB values vary from pixel to pixel as to which value is highest. The red and green values vary slightly from layer to layer, because the pixel values are measured manually for each layer, and so the exact spot within in pixel measured varies.

For the silicon layer stack, blue is always highest, with a mean of 235; red is usually higher than green, with a mean of 167 and 136 respectively. The iron layer stack is a little less blue with a mean of 189, and red and green means of 167 and 137 respectively. For both the Si and Fe layer stacks, there is less of a north south division.

	R	G	B	R	G	B	R	G	B
zone	Cl	H	K/Th	Cl	H	K/Th	Cl	H	K/Th
nc	179	190	79	180	189	247	179	189	221
nc	167	186	111	168	187	246	167	187	207
nc	158	173	123	157	173	231	158	174	190
nc	151	209	193	152	210	241	151	210	189
nc	140	161	135	140	161	233	158	174	190
ne	175	179	135	175	179	233	175	180	195
ne	150	154	87	150	153	247	149	154	195
ne	140	131	181	140	130	236	139	131	199
ne	135	138	186	136	138	238	134	138	192
sc	149	110	52	150	109	246	149	110	184
sc	145	88	52	145	88	248	146	89	187
sc	140	118	59	143	119	230	141	120	172
sc	142	151	61	142	151	237	142	150	182

zone	Cl	H	K/Th	Cl	H	K/Th	Cl	H	K/Th
sc	136	121	143	135	122	237	135	121	173
se	209	133	75	211	132	230	210	134	200
se	209	133	75	211	132	230	210	134	200
se	209	133	75	211	132	230	210	134	200
se	198	136	98	198	135	231	198	135	196
se	188	129	91	187	129	230	187	129	188
se	188	129	91	187	129	230	187	129	188
se	182	138	108	181	139	232	182	138	180
se	174	134	92	173	133	238	174	133	182
se	149	149	72	150	148	240	149	148	186
sw	174	106	74	175	103	230	175	107	187
sw	174	106	74	175	103	230	175	107	187
sw	174	106	74	175	103	230	175	107	187
sw	170	119	70	170	119	231	169	120	185
sw	171	125	69	169	125	231	170	124	180
sw	171	125	69	169	125	231	170	124	180
sw	167	111	67	168	112	228	169	111	186
sw	162	129	81	163	128	227	163	129	180
sw	162	129	81	163	128	227	163	129	180
sw	164	127	92	162	128	231	163	129	181
mean	167	137	95	167	136	235	167	137	189

Figure 17 is an overlay of the geologic history periods of Mars, grouped into 5 broad time periods, and the 33 high gully locations. Twenty four out of 33 high gullies are either Noachian-Hesperian or Noachian, the two oldest time periods.

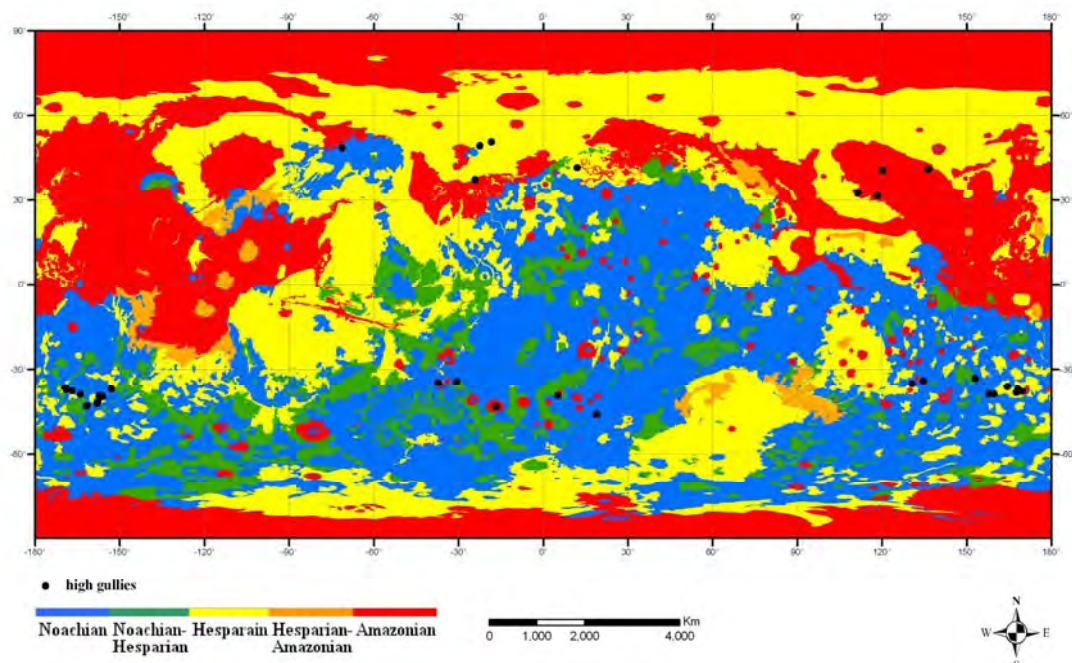


Figure 17. Gullies and Geology. High gullies and five broad geologic time periods of Mars. Ages are adapted from the USGS Martian Geologic Investigations Series I-1802 (ABC) Scott and Tanaka (1986), Greeley and Guest (1987), and Tanaka and Scott (1987); and Hahn et al. (2007, 3).

Branching Ratios

Both high drainage densities and branching ratios imply older gullies. High correlation coefficients for water concentration sites vs. branching ratio imply a strong correlation between water and gullies. The concentration of other elements may also imply the presence of water. For example low silicon or iron concentrations may imply these elements have been leached. Furthermore low K/TH ratios may imply K has been leached, whereas a high chlorine concentration may imply the presence of brine. The mere location of gullies in areas of high hydrogen concentration and low concentration of other elements, such as potassium, iron, and silicon may also imply the presence of water. Figure 18 is a typical image with an overlay of digitized gullies. The digitization better visualizes the gully structure, and aids in the counting of the branches.

The image in Figure 18 has a typical badlands with the gully channels digitized, and the data in Table 5 and Figures 19-21 are the results for all of the high gullies. The data in Table 5 contains R^2 values significantly less than 0.1. Furthermore the graphs in Figures 19-21, with the exception of chlorine, have slopes near 0. These data imply there is no correlation between element concentrations and gully formation.

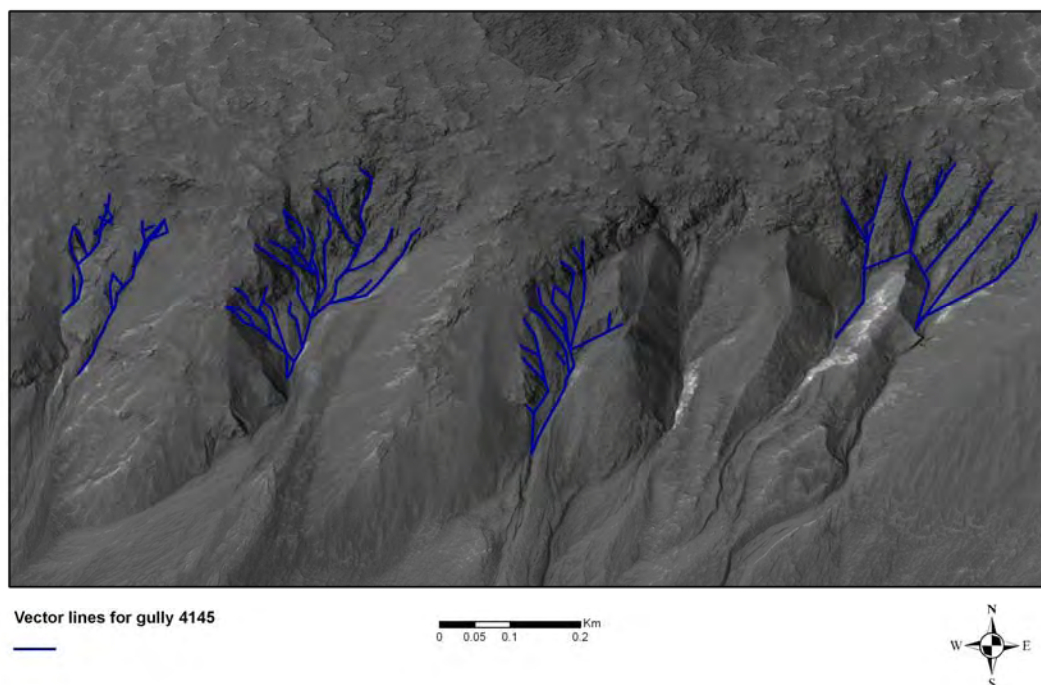


Figure 18. A typical MRO image with the gullies digitized. Gully branches are blue for easier viewing.

Table 5. Branching Ratio vs. water and various elements		
element	R	R^2
water	0.074	0.006
Cl	0.225	0.051
K/Th	0.042	0.002
Fe	0.052	0.003
Si	0.046	0.002

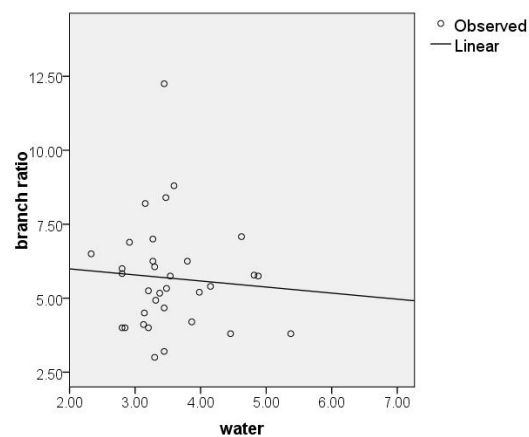
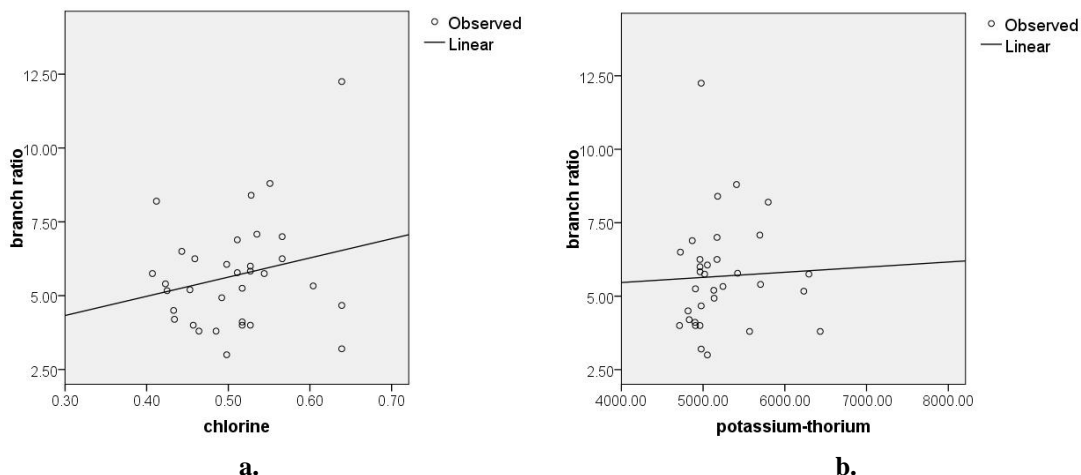
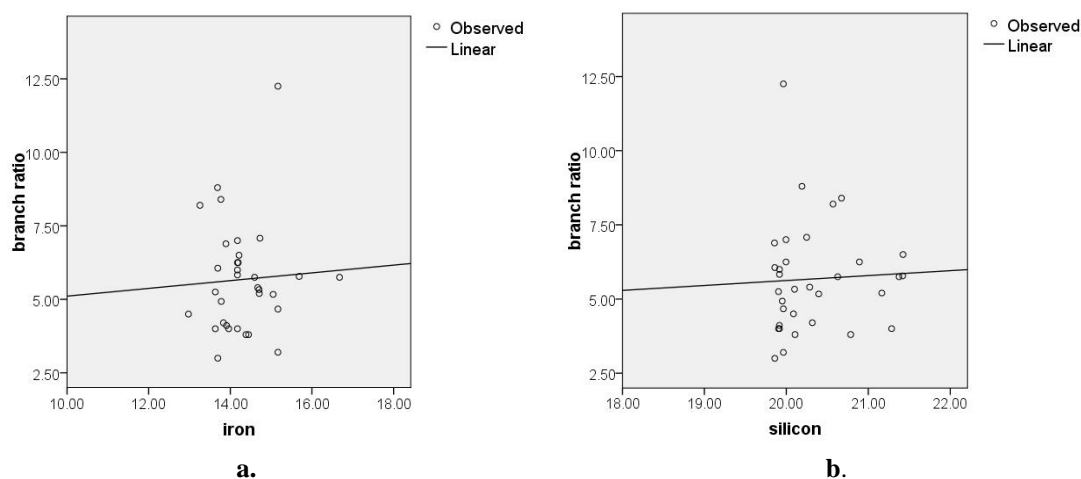


Figure 19. 33 High Gullies Branching Ratio vs. water concentration
 $y = -0.205x + 6.400$.



**Figure 20. High Gully Branching Ratio vs. concentration a. chlorine $y = 2.380x + 6.497$.
b. K/Th $y = 0.000x + 4.767$.**



**Figure 21. High Gully Branching Ratio vs. concentration a. Fe $y = 0.132x + 3.791$.
b. Si $y = 0.166x + 2.295$**

Decision Tree

For the first set of decision tree iterations, the process produced different trees on each iteration. The most complicated tree produced (having the most nodes and depth), is shown in Table 6. Fe, K/Th, water, and Cl are all independent variables that show up in the resulting tree, shown in Figure 22. The test set size is 40% of the total points. The resultant tree has 13 nodes, 8 of which are terminal, and a depth of 3. High gullies are most likely (10 out of 12 or 83%) found in node 6, areas with an iron concentration

between 12.96% and 14.71%, and a water concentration less than 4.57%. Similarly, 60% of low branching gullies are found in the same locations. In contrast only 3 out of 12 random GIS sites are found in the same locations. These results indicate chlorine, iron and water are predictors of gully formation. It should also be noted that both chlorine and iron are often salt and brine components.

Specifications	Growing Method	CHAID
	Dependent Variable	type (high)
	Independent Variables	water, chlorine, potassium-thorium, iron, silicon, geology
	Validation	Split Sample training 60% test 40%
	Maximum Tree Depth	3
	Minimum Cases in Parent Node	2
	Minimum Cases in Child Node	1
Results	Independent Variables Included	iron, potassium-thorium, water, chlorine
	Number of Nodes	13
	Number of Terminal Nodes	8
	Depth	3

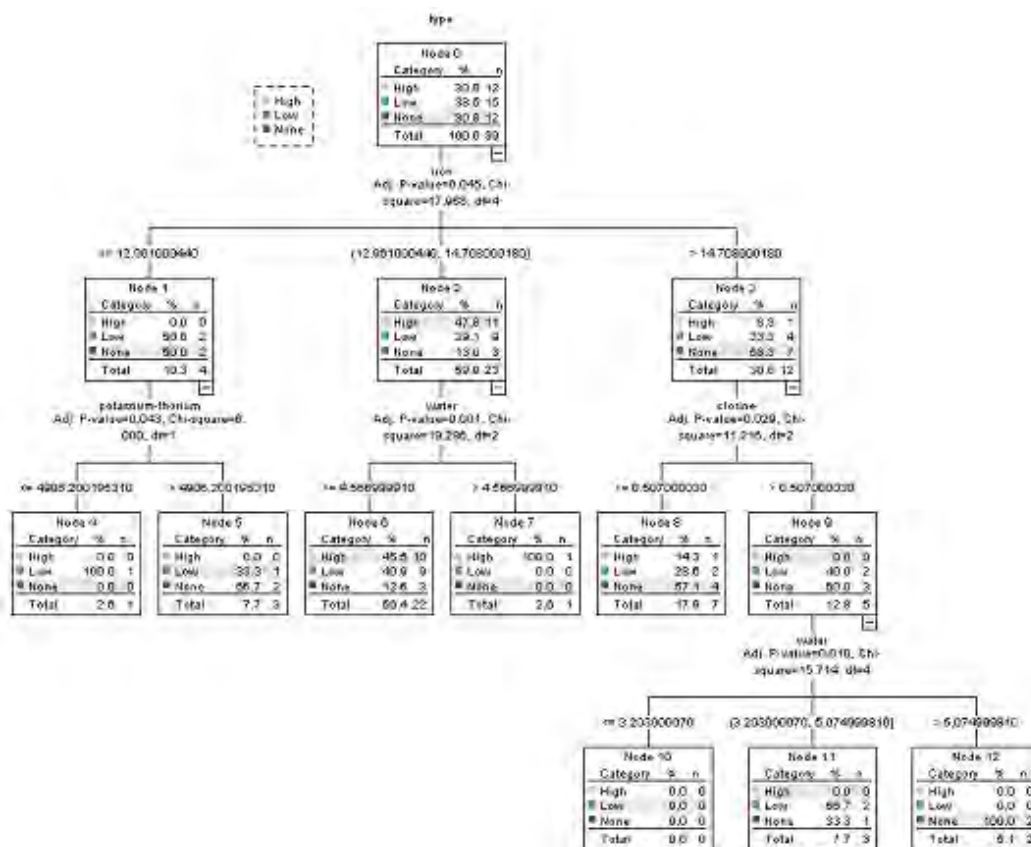


Figure 22. Decision tree. (Iteration 1) Graphical representation of a robust decision tree.

Table 7 is the risk table for this decision tree process. The estimated value is the proportion of wrong predictions for the whole model. This iteration has a 56.4% proportion for the test sample. However Table 8, the classification table, shows an 83.3% correct prediction of what is a high gully. The model incorrectly identifies 11 out of 15 low gullies as high gullies, and correctly identifies half of the random points as random points.

Table 7. Decision Tree Risk (Iteration 1)		
Sample	Estimate	Standard Error
Training	.283	.058
Test	.564	.079

Sample	Observed	Predicted			
		High	Low	None	Percent Correct
Training	High	21	0	0	100.0%
	Low	12	3	3	16.7%
	None	2	0	19	90.5%
	Overall Percentage	58.3%	5.0%	36.7%	71.7%
Test	High	10	0	2	83.3%
	Low	11	1	3	6.7%
	None	4	2	6	50.0%
	Overall Percentage	64.1%	7.7%	28.2%	43.6%

For the second set of decision trees, longitude and latitude are added as independent variables. Table 9 contains the summary, and Figure 23 contains this decision tree. Latitude, chlorine, and longitude are the independent variables affecting the tree. The tree has a depth of three with 12 nodes, seven of which are terminal. Seventy percent of the sample is used for training.

Specifications	Growing Method	CHAID
	Dependent Variable	type (high)
	Independent Variables	longitude, latitude, water, chlorine, iron, geology, potassium-thorium
	Validation	Split Sample training 70% test 30%
	Maximum Tree Depth	3
	Minimum Cases in Parent Node	2
	Minimum Cases in Child Node	1
Results	Independent Variables Included	latitude, chlorine, longitude
	Number of Nodes	12
	Number of Terminal Nodes	7
	Depth	3

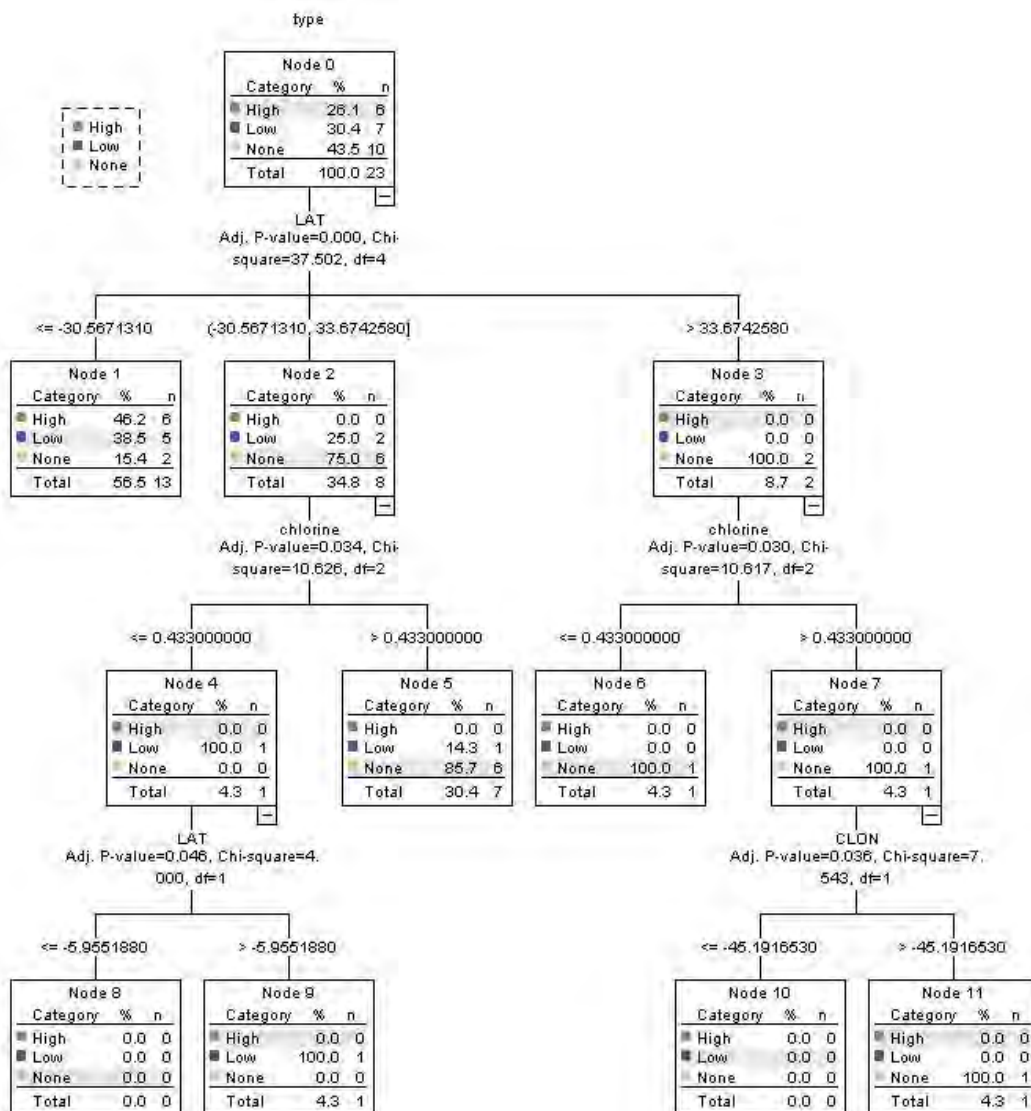


Figure 23. Decision Tree. (Iteration 2) Graphical representation of a SPSS decision tree. LAT: latitude CLON: longitude

Table 10 is the risk table for this decision tree process. The estimated value is the proportion of wrong predictions for the whole model. This iteration has a 47.8% proportion for the test sample Here again the model confuses high and low gullies, by identifying all of the high gullies as low gullies, while 70% of the random points are identified as random points, as seen in Table 11. The frequent false identification of low gullies as high gullies and visa versa implies the low and high gullies have very similar environments.

Sample	Estimate	Std. Error
Training	.329	.054
Test	.478	.104

Sample	Observed	Predicted			Percent Correct
		High	Low	None	
Training	High	8	18	1	29.6%
	Low	1	22	3	84.6%
	None	0	2	21	91.3%
	Overall Percentage	11.8%	55.3%	32.9%	67.1%
Test	High	0	6	0	.0%
	Low	1	5	1	71.4%
	None	1	2	7	70.0%
	Overall Percentage	8.7%	56.5%	34.8%	52.2%

Chapter 5

CONCLUSIONS

Nearest Neighbor and Euclidean distance tests are performed to determine the spatial distribution of gullies. Nearest neighbor ratios of 0.47 and 0.85 for high and low gullies respectively and several large Euclidean Distance areas greater than 45° for both high and low gullies indicate both the low and high gullies are clustered. Twenty three out of thirty three low gullies appear in an area stretching from 90° to -150° longitude between -30° and -45° latitude. The other ten low gullies appear dispersed, with no more than two low gullies within 30° of one another. Nineteen of the high gullies also appear in the same southern region as most of the low gullies. The high gullies are also clustered in three other areas: five in a south central zone, five in a north central zone, and four in a northeastern zone. Both nearest neighbor ratio and Euclidean distances indicate the randomly created GIS points are in fact random.

Findings indicate the surface of Mars has a patch work of concentrations of elements, and both the southern low and high gullies are found in areas high in chlorine, low in water, low K/Th, low Fe, and even lower Si. One very interesting spatial aspect of this data is that there are no gullies in the largest heavily water rich area in the center of the maps seen in Figures 18 - 20. In fact, few gullies are found within 30° of the equator. One possible explanation may be the water flow models presented by Clancy (1996) and

Kuzmin (2006), and others, in which water is transported from the equator to the polar regions where it eventually condenses and mixes with other minerals. Figure 21 shows geologic patchwork. As one might expect most of the gullies are located in geologically older eroded areas.

The decision tree data indicates chlorine and latitude as the prime determinants as to where gullies are located. I am surprised geology is not also a determinant. A possible explanation why geology is not a determinant in the decision tree is that when creating the map in Figure 21, I decided to create five periods rather than three. A three period map of Amazonian, Hesperian, and Noachian would likely make Noachian a determinant.

The GRS data and the decision trees corroborate the presence of high concentrations of chlorine and other elements. The presence of high concentrations of elements—in particular chlorine—points to brine as the primary liquid source of gullies on Mars. The decision trees also suggest the high and low gullies are one and the same. For future research I would like to map all of the nearly 500 gullies identified in HiRISE images.

Unfortunately the linear regression results in Table 3 and Figures 12 -14 imply no correlation between any GRS data and branching ratio. One possible explanation is the resolution of the GRS is $5^\circ \times 5^\circ$ (296 km x 295 km at the equator). A typical gully is less than 500 m in width and length, and so the resolution is too coarse.

The advocates of the CO₂, dry flow, and water seepage present strong evidence favoring their views. Figure 3a would appear to be an example of the outcome of the cryoclastic model presented in Figure 7 by (Hoffman 2000), and the white outcroppings in Figure 3b may very well be water ice. Pelletier et al. (2008) also make a strong case for

dry, as seen in Figure 8. However the scope of this thesis involves using GIS, remote sensing, and decision tree to analyze images and elemental data. Both elemental and decision tree results support the presence of both iron and chlorine as determinants of gully formation, and Bridges and Grady (1999) and Grady (2005) both have found these elements in Martian salts. My research therefore strongly points to brine as the fluid source for most gullies on Mars. However some gullies may have other fluid sources.

REFERENCES

- Andersen, Dale T., Wayne H. Pollard, Christopher P. McKay, and Jennifer Heldmann. 2002. Cold springs in permafrost on Earth and Mars. *Journal of Geophysical Research* 107, no. E3, 5015, 10.1029/2000JE001436: 1-7.
- ASU. <http://themis.asu.edu/mars-bin/webmap.pl>. accessed May 3, 2006.
- Balme, Matthew. R., Nicholas Mangold, David Baratoux, Francis Costard, Matthieu Gosselin, Philippe Masson, Patrick Pinet, and Gerhard Neukum. 2006. Orientation and distribution of recent gullies in the southern hemisphere of Mars: Observations from High Resolution Stereo Camera/Mars Express (HRSC/MEX) and Mars Orbiter Camera/Mars Global Surveyor (MOC/MGS) data. *Journal of Geophysical Research* 111, no. E05001: 1-20.
- Bourke, M. C., M. Balme, R. A. Beyer, K. K. Williams, and J. Zimbelman. 2006. A comparison of methods used to estimate the height of sand dunes on Mars. *Geomorphology*. 81: 440-452.
- Boynton, W. V. et al. 2007. Concentration of H, Si, Cl, K, Fe, and Th in the low- and mid-latitude regions of Mars. *Journal of Geophysical Research* 112, no. E12S99: 1-15.
- Bridges, J. C. and M. M. Grady. 1999. A halite-siderite-anhydrite-chlorapatite assemblage in Nakhla: Mineralogical evidence for evaporites on Mars. *Meteoritics and Planetary Science*, v. 34(3), p. 407-415.
- Bridges, Nathan T. and Claire N. Lackner. 2006. Northern hemisphere Martian gullies and mantled terrain: Implications for near surface water migration in Mars' recent past. *Journal of Geophysical Research*, 111, E09014: 1-20.
- Bryson, Kathryn L., Vincent Chevrier, Derek W. G. Sears, and Richard Ulrich. 2008. Stability of ice on Mars and the water vapor diurnal cycle: Experimental study of the sublimation of ice through a fine-grained basaltic regolith. *Icarus* 196: 446-458.
- Chapman, Mary, ed. *The Geology of Mars: Evidence from Earth-based Analogs*. Cambridge: Cambridge University Press, 2007.
- Christensen, Philip R. 2003. Formation of recent Martian gullies through melting of extensive water-rich snow deposits. *Nature (London)* 422, no. 6927: 45-48.
- Clancy, R. T., A. W. Grossman, M. J. Wolff, P. B. James, D. J. Rudy, Y. N. Billawala, B. J. Sandor, S. W. Lee, and D. O. Muhleman. 1996. Water Vapor Saturation

- at Low Altitudes around Mars Aphelion: A Key to Mars Climate?. *Icarus* 122: 36–62.
- Frey, E. L., S. E. H. Sakimoto, and H. V. Frey. 2004. A preliminary relationship between the depth of Martian gullies and the abundance of hydrogen on near-surface Mars. *Lunar and Planetary Institute Conference Abstracts* 35: 1977-1978.
- Gabet, Emmanuel J. and Andy Bookter. 2008. A morphometric analysis of gullies scoured by post-fire progressively bulked debris flows in southwest Montana, USA. *Geomorphology* 96: 298–309.
- Greeley, Ronald and John E. Guest. I-1802-B: *Geologic Map of the Eastern Equatorial Region of Mars*. Flagstaff: USGS 1987.
- Hahn, Brian C. et al. 2007. Mars Odyssey Gamma Ray Spectrometer elemental abundances and apparent relative surface age: Implications for Martian crustal evolution. *Journal of Geophysical Research* 112, no. E03S11: 1-13.
- Hartmann, William K. 2001. Martian seeps and their relation to youthful geothermal activity. *Space Science Reviews* 96: 405-410.
- Hartmann, William K., Thorsteinn Thorsteinsson, and Freysteinn Sigurdsson. 2003. Martian hillside gullies and Icelandic analogs. *Icarus* 162, 259–277.
- Heldmann, Jennifer L. and Michael T. Mellon. 2004a. Gullies on Mars and constraints imposed by Mars global surveyor data. *Lunar and Planetary Institute Conference Abstracts* 35: 1355-1356.
- Heldmann, Jennifer L. and Michael T. Mellon. 2004b. Observations of Martian gullies and constraints on potential formation mechanisms. *Icarus* 168, no. 2: 285-304.
- Hoffman, Nick. 2000. White Mars: A new model for Mars' surface and atmosphere Based on CO₂. *Icarus* 146, 326–342.
- Hyde, Kevin, Scott W. Woods, and Jack Donahue. 2007. Predicting gully rejuvenation after wildfire using remotely sensed burn severity data. *Geomorphology* 86: 496–511.
- Ishii, T., H. Miyamoto, S. Sasaki, and E. Tajika 2006. Constraints on the formation of gullies on MARS: A possibility of the formation of gullies by avalanches of granular CO₂ ice. *37th Annual Lunar and Planetary Science Conference* 37: 1646-1647.
- Jagoutz, Emil. 2006. Salt-induced rock fragmentation on Mars: The role of salt in the weathering of Martian rocks. *Advances in Space Research* 38: 696-700.
- JPL. <http://marsprogram.jpl.nasa.gov/missions/log/>. accessed March 21, 2009.

- Kuzmin, R. O., E. V. Zabalueva, I. G. Mitrofanov, M. L. Litvak, A. V. Rodin, W. V. Boynton, and R. S. Saunders. 2007. Seasonal Redistribution of Water in the Surficial Martian Regolith: Results from the *Mars Odyssey* High-Energy Neutron Detector (HEND). *Solar System Research* 41, no. 2: 89-102.
- Lanza, Nina L. and Martha S. Gilmore. 2006. Depths, orientation and slopes of Martian hillside gullies in the northern hemisphere. *37th Annual Lunar and Planetary Science Conference* 37: 2412-2413.
- Lee, Pascal, Brian J. Glass, Gordon R. Osinski, John Parnell, John W. Schutt, and Christopher P. McKay. 2006. Gullies on mars: Fresh gullies in dirty snow, Devon Island, high arctic, as end-member analogs. *37th Annual Lunar and Planetary Science Conference* 37: 1818-1819.
- Lowell, Percival. *Mars And Its Canals*. Norwood: Norwood Press, 1906.
- Malin, Michael C. and Kenneth S. Edgett. 2000. Evidence for recent groundwater seepage and surface runoff on Mars. *Science* 288, no. 5475: 2330-2335.
- Martel, Linda M. V. 2003. *Gullied Slopes on Mars*. Honolulu, HI Planetary Science Research Discoveries. August 2003: 1-5.
- Mellon, Michael T. and Roger J. Phillips. 2001. Recent gullies on Mars and the source of liquid water. *Journal of Geophysical Research* 106, no. E10: 23165-23179.
- Mohan, Swati and Nathan T. Bridges. 2004. Analysis of orientation-dependence of Martian gullies. *Lunar and Planetary Institute Conference Abstracts* 35: 1339-1340.
- Musselwhite, Donald S., Timothy D. Swindle, and Donathan I. Lunine. 2001. Liquid CO₂ Breakout and the Formation of Recent Small Gullies on Mars. *Geophysical Research Letters* vol. 28, no. 7: 1283-1285.
- Pelletier, Jon D., Kelly J. Kolb, Alfred S. McEwen, and Randy L. Kirk. 2008. Recent bright gully deposits on Mars: Wet or dry flow?. *Geology*. March 2008: 211-214.
- Rijsdijk, Anton, L.A. (Sampurno) Bruijnzeel, and T. M. Prins. 2007. Sediment yield from gullies, riparian mass wasting and bank erosion in the Upper Konto catchment, East Java, Indonesia. *Geomorphology* 87: 38-52.
- Roa, M. N., S. R. Sutton, D. S. McKay, and G. Dreibus. 2005. Clues to Martian brines based on halogens in salts from nakhlites and MER samples. *Journal of Geophysical Research* 110, no. E12S06: 1-12.

- Scott, David H. and Kenneth L. Tanaka. I-1802-A: *Geologic Map of the Western Equatorial Region of Mars*. Flagstaff: USGS 1986.
- Tanaka, Kenneth L. and David H. Scott. I-1802-C: *Geologic Map of the Polar Regions of Mars*. Flagstaff: USGS 1987.
- Taylor, G. Jeffrey et al. 2006a. Variations in K/Th on Mars. *Journal of Geophysical Research* 111, no. E03S06: 1-20.
- Taylor, G. Jeffrey et al. 2006b. Bulk composition and early differentiation of Mars. *Journal of Geophysical Research* 111, no. E03S10: 1-20.
- Touma, Jihad and Jack Wisdom. 1993. The Chaotic Obliquity of Mars. *Science* 259, no. 5099: 1294-1296.
- Treiman, Allan. 2003. Geologic settings of Martian gullies: Implications for their origins. *Journal of Geophysical Research* 108, no. E4 8031: 1-13.
- USGS. <http://isis.astrogeology.usgs.gov/documents/Overview/Overview.html> accessed May 3, 2006a.
- USGS. <http://ida.wr.usgs.gov/graphical.htm> accessed May 3, 2006b.
- WUS. <http://pds-geosciences.wustl.edu/missions/mgs/megdr.html> accessed May 3, 2006.

VITA

Leon Kincy was born Leondres Kincy III into an Air Force family, and grew up throughout the U.S., Japan, and England. He graduated from Leander High School. He obtained a B.A. degree in Computer Science May, 1998 from then Southwest Texas State University and a B.S. in Geography from Texas State University-San Marcos in August, 2005. He worked for the Texas Department of Public Safety for 17 years and currently works for the Texas Department of State Health Services.

Permanent Address:

PO Box 8277

Austin, TX 78713

This thesis was typed by Leon Kincy.